



Simulation of the Laptev Sea shelf dynamics with focus on the Lena Delta region

V. Fofonova¹, S. Danilov¹, A. Androsov¹, P. Overduin¹ and K.H. Wiltshire¹
¹Alfred Wegener Institute, Helmholtz Centre for Polar and Marine Research

IMUM2014, 27th of August, 2014

Content

Motivation

I. Model setup

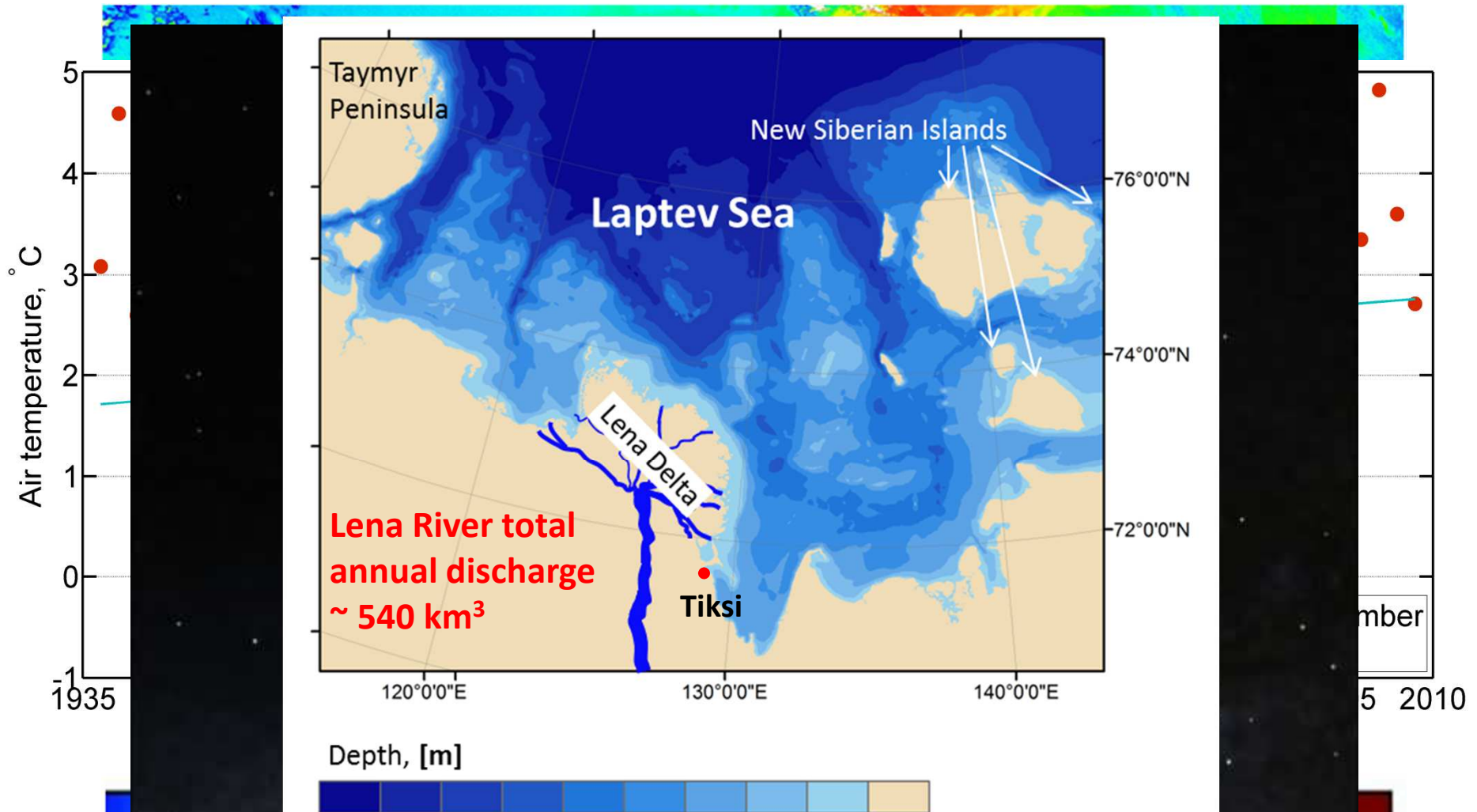
II. Study of barotropic tidal dynamics

III. Lena River hydrological module

IV. Study of full baroclinic dynamics with focus on
the Lena River freshwater plume propagation

Summary

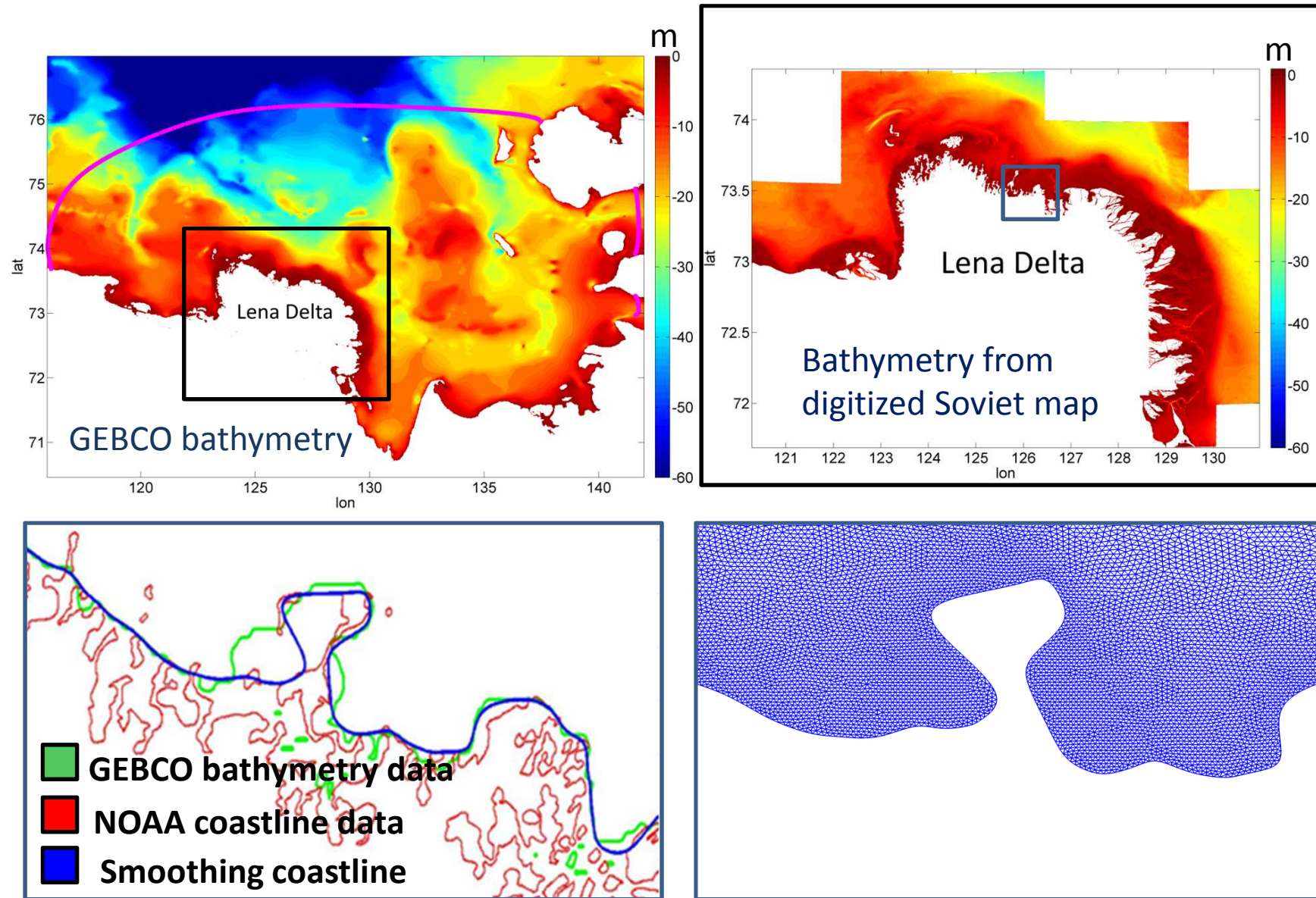
Motivation



Mean surface air temperature from 1936 to 2009, Tiksi Bay. The theoretical slope of the line is significantly different from 0 with **98% probability**.

Total Suspended Matter (TSM), g m^{-3} , late summer, 2011

Model domain



Porting FVCOM

FVCOM - Finite Volume Coastal/Community Ocean Model (Chen et al., 2006)

- 11 vertical sigma layers, 256479 nodes/per layer
- Horizontal resolution: from 0.4 to 5 km
- External/internal time steps: 3.6/36 s
- Open boundary: temperature/salinity time series nudging
- Vertical and horizontal mixing simulation: Mellor and Yamada level 2.5 and Smagorinsky turbulent closure schemes, respectively

Initial conditions and forcing

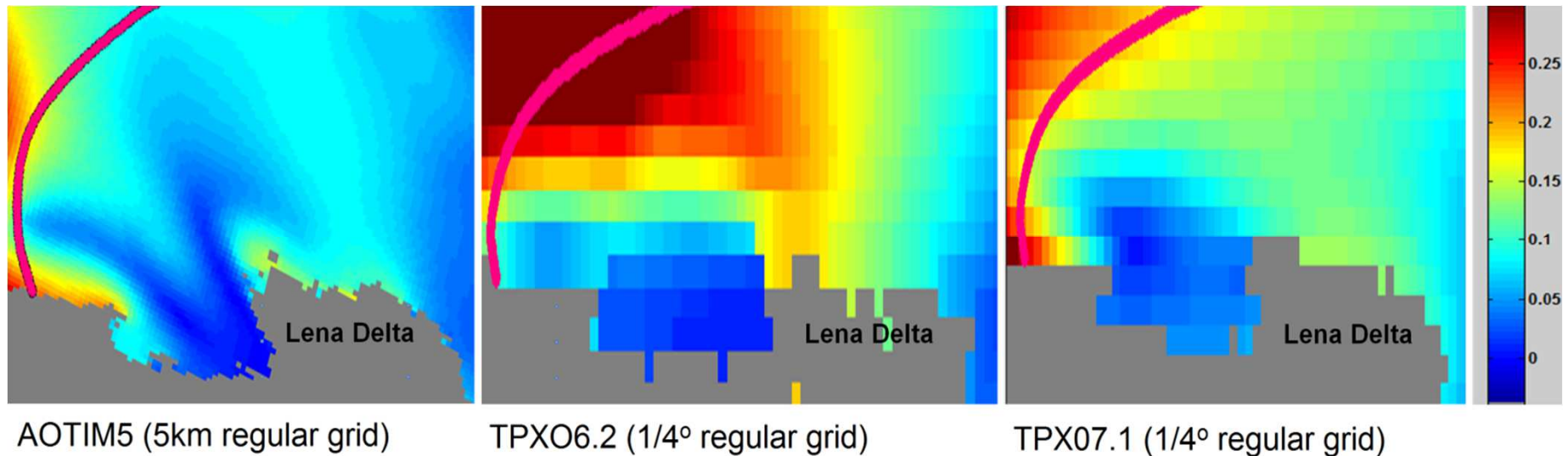
- **Bathymetry and coastline data** – NOAA, GEBCO and the digitized Soviet map
- **Atmospheric data** – COSMO model (University of Trier), NCEP Reanalysis 2 and ECMWF atmospheric model
- **Initial salinity and temperature fields** – a coupled Sea/Ice Ocean model (NAOSIM, AWI Bremerhaven)
- **Tidal elevation at the open boundary** – TPXO6.2, TPXO7.1, AOTIM5 and optimal open boundary conditions
- **Runoff data/Temperature of runoff** – observational data from Kusur station

Semidiurnal tides in the Laptev Sea shelf zone

The main issues:

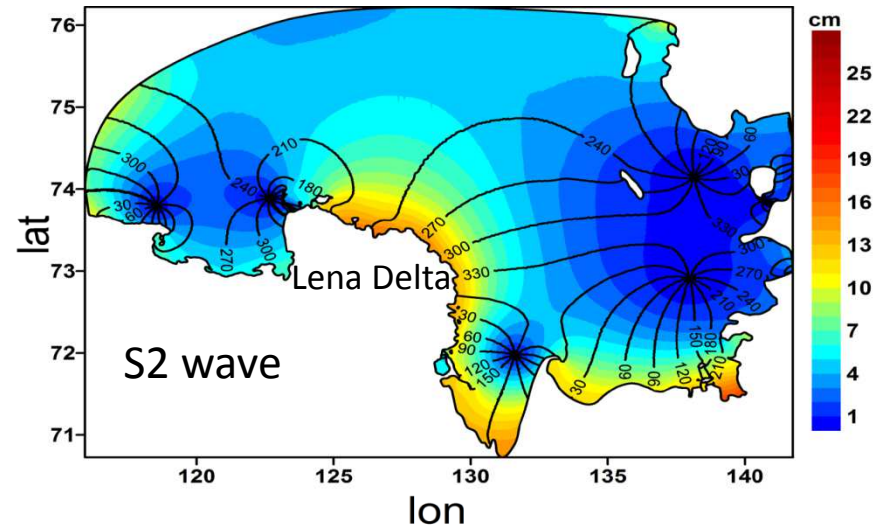
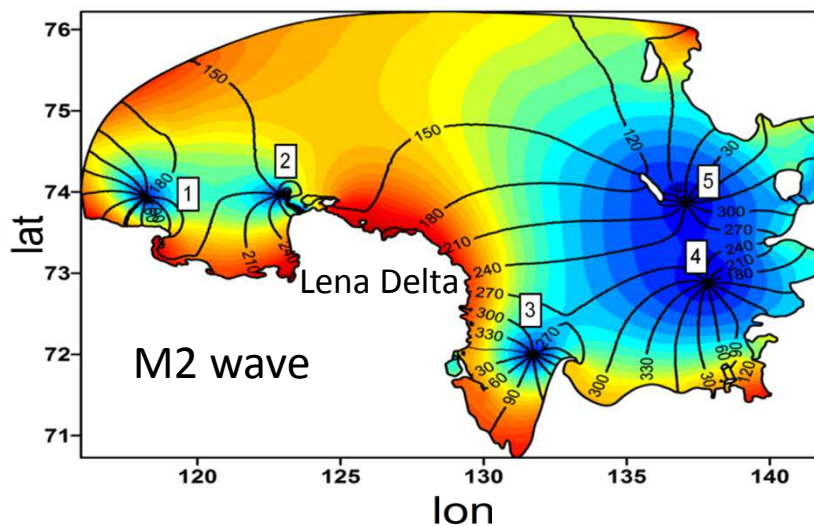
1. To specify boundary conditions
2. To resolve bathymetry features

Available tidal solutions

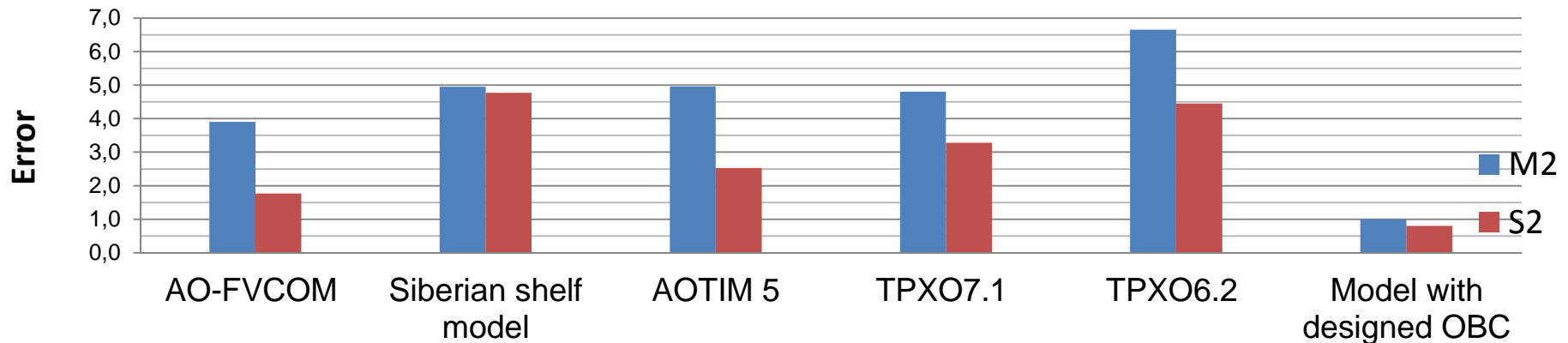


Amplitude, [m], of the M2 constituent in the Lena Delta region of the Laptev Sea. The maps are obtained using TMD toolbox provided by Erofeeva and Padman, 2004.

Tidal maps for M2, S2 waves

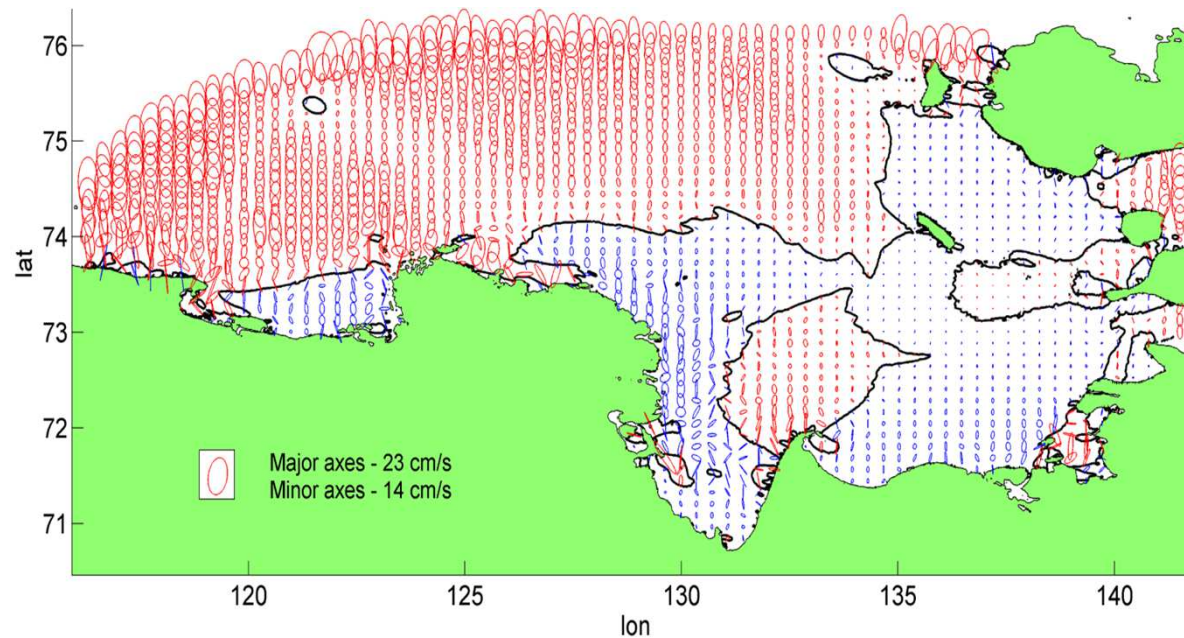


Results of simulation with optimal designed open boundary conditions for tidal elevation.



RMS error, [cm], obtained from different models compare to coastal tide gauges (**10 stations**).
AOTIM5, TPX07.1, TPX06.2 – models with data assimilation.

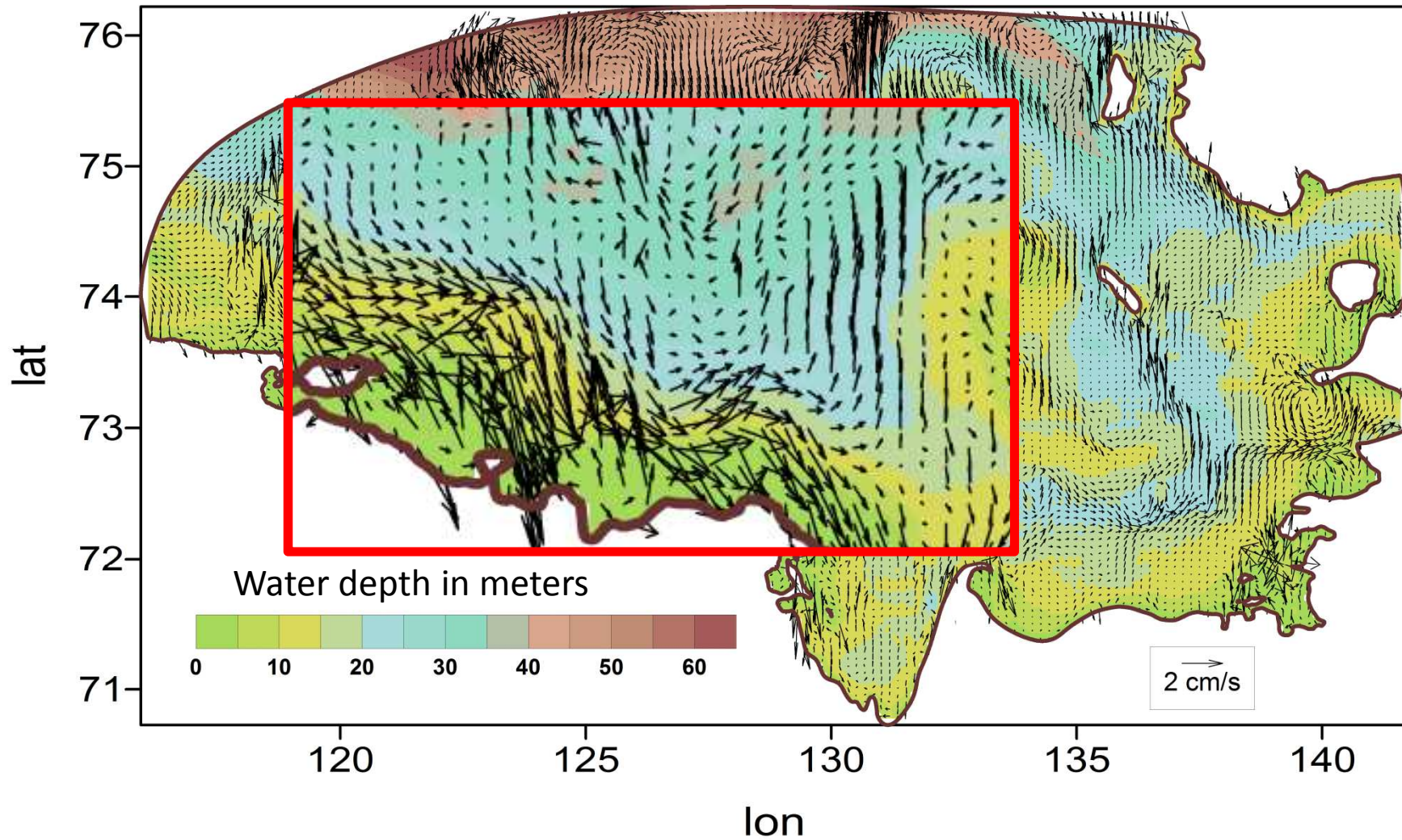
Tidal ellipses



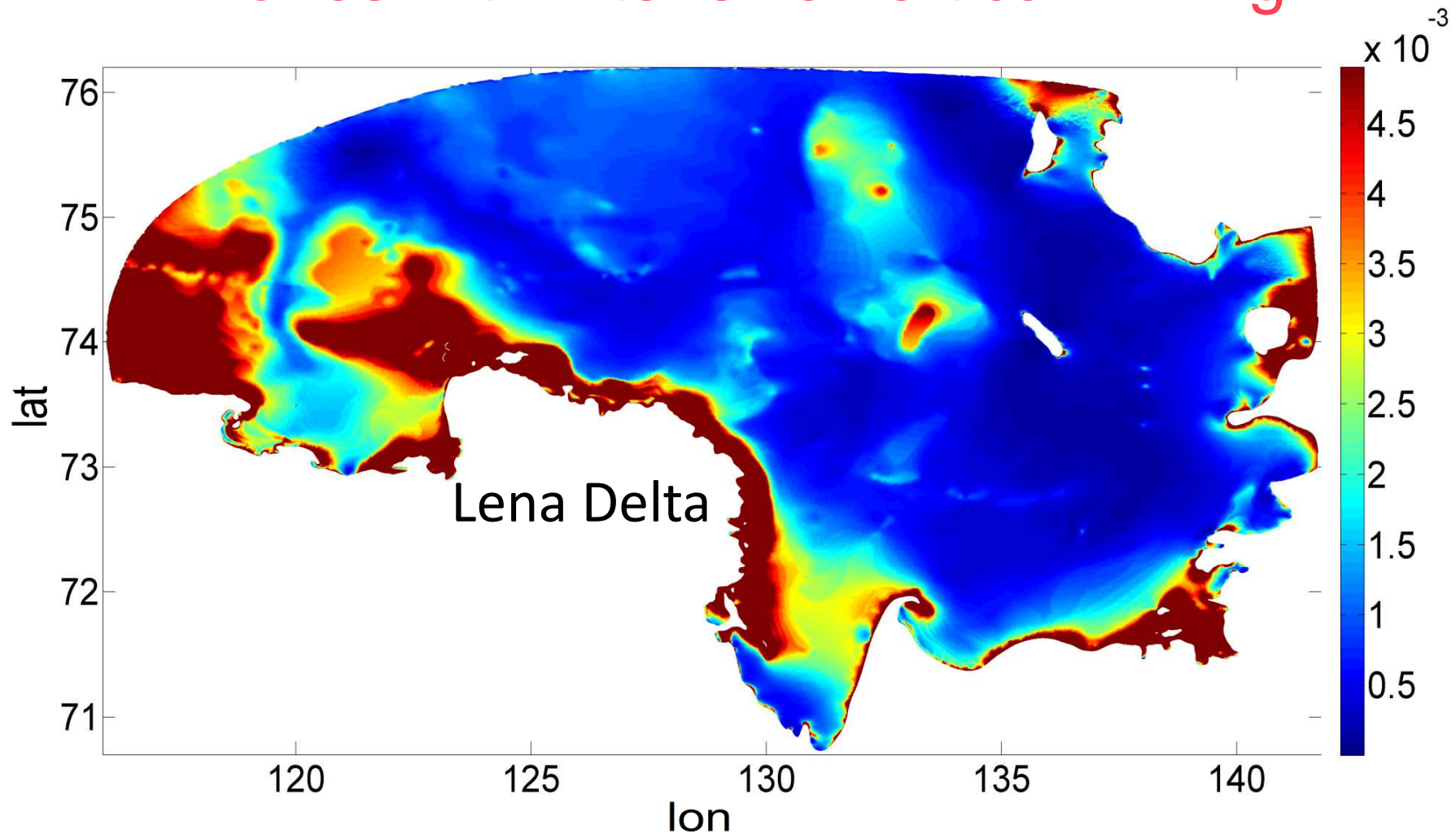
Ellipses of barotropic velocities for the M2 tide, red ellipses have CW rotation, blue ellipses have CCW rotation.

Comparison of ellipse parameters with AWI moorings data (5 stations) for M2(S2) waves				
Solution	AOTIM5	TPX07.1	TPX06.2	Model with OOBC
Ellipse parameters				
Error_major axes, [cm/s]	6.3(4.1)	4.7(2.7)	2.9(3.9)	1.4(1.5)
Error_minor axes, [cm/s]	1.2(1.3)	2.3(0.9)	2.8(3.3)	3.2(2)

Residual circulation for summary tide



Zones with intensive vertical mixing

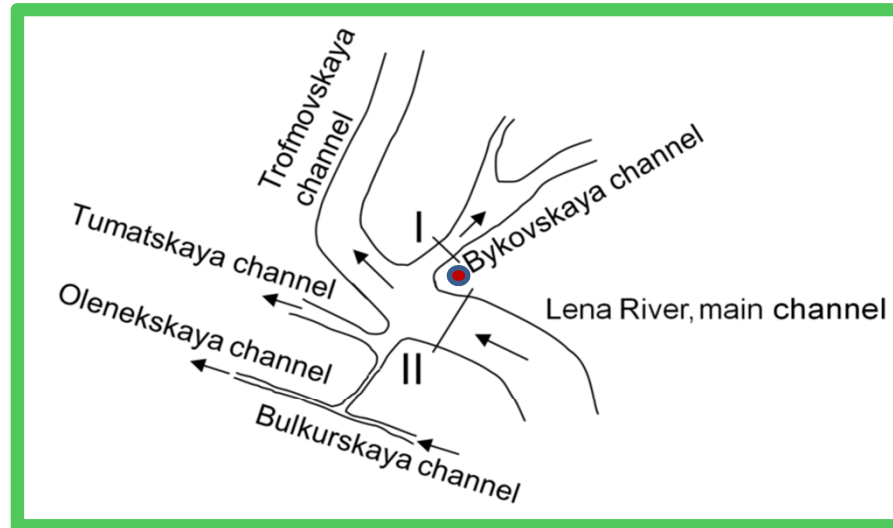


Mean vertical shear, $[1/s]$, generated by M2 wave at the moment of maximum kinetic energy.

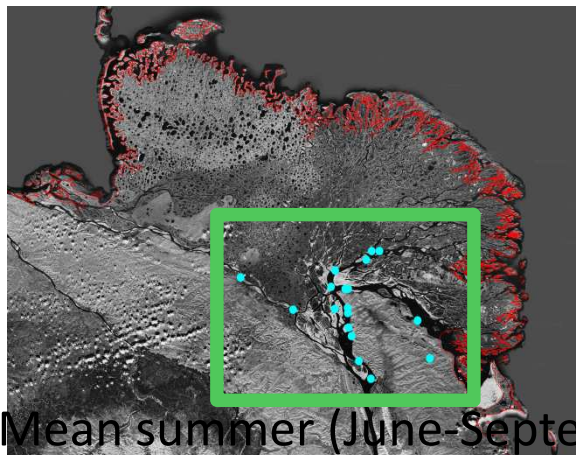
Creating the Lena River hydrological module

Development of the:

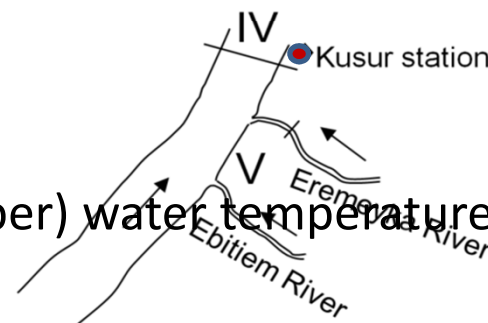
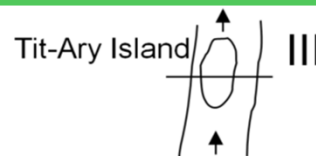
- 1) Hydrological database
- 2) Module, which predicts the Lena River temperature in the mouth area



- I – GS Habarova (Stolb, Bykovskaya channel)
- II – GS Stolb, main channel
- III – GS Tit-Ary
- IV – GS Kusur
- V – GS Eremeyka

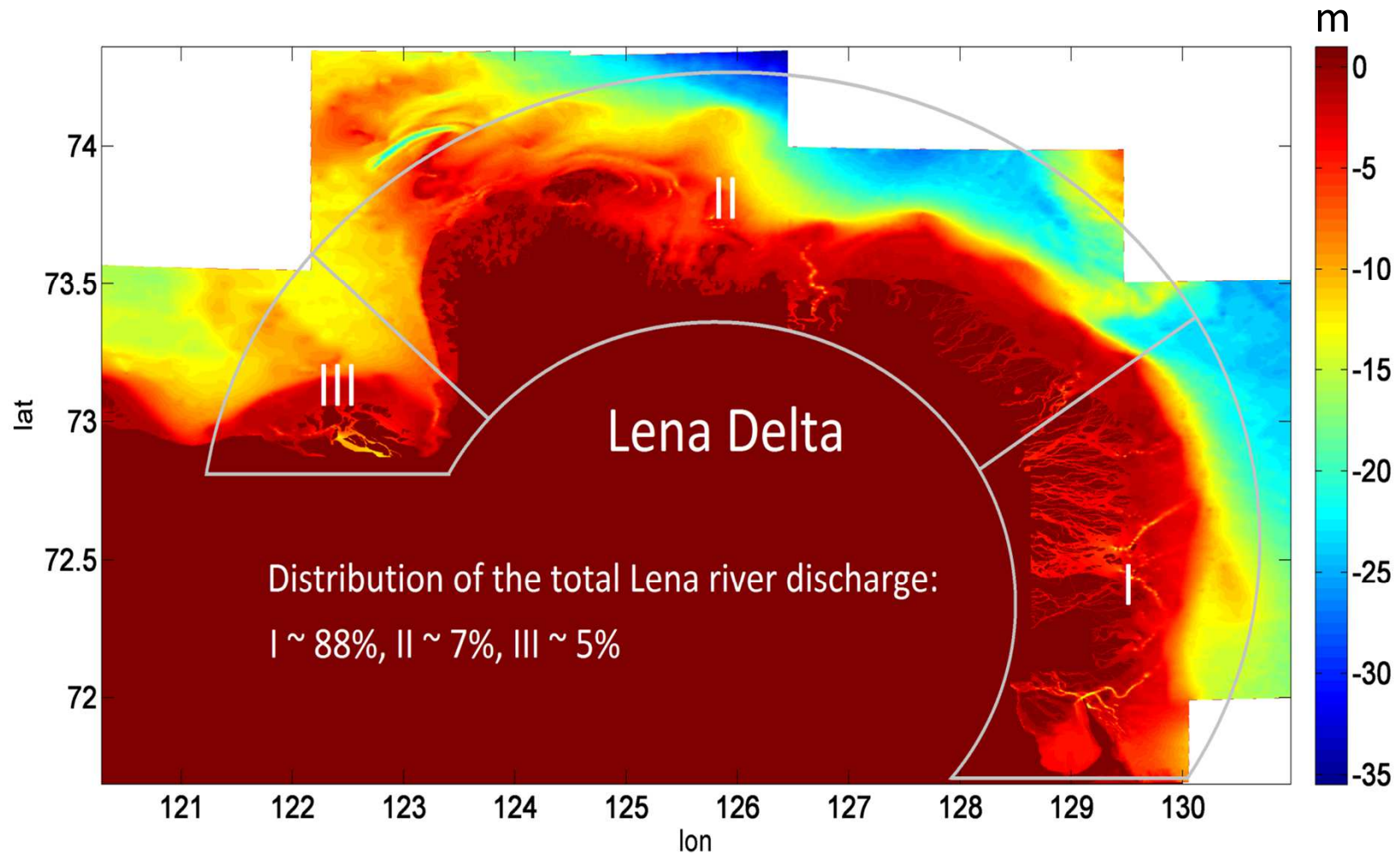


Mean summer (June-September) water temperature at gauging stations (GS) Kusur and Habarova.

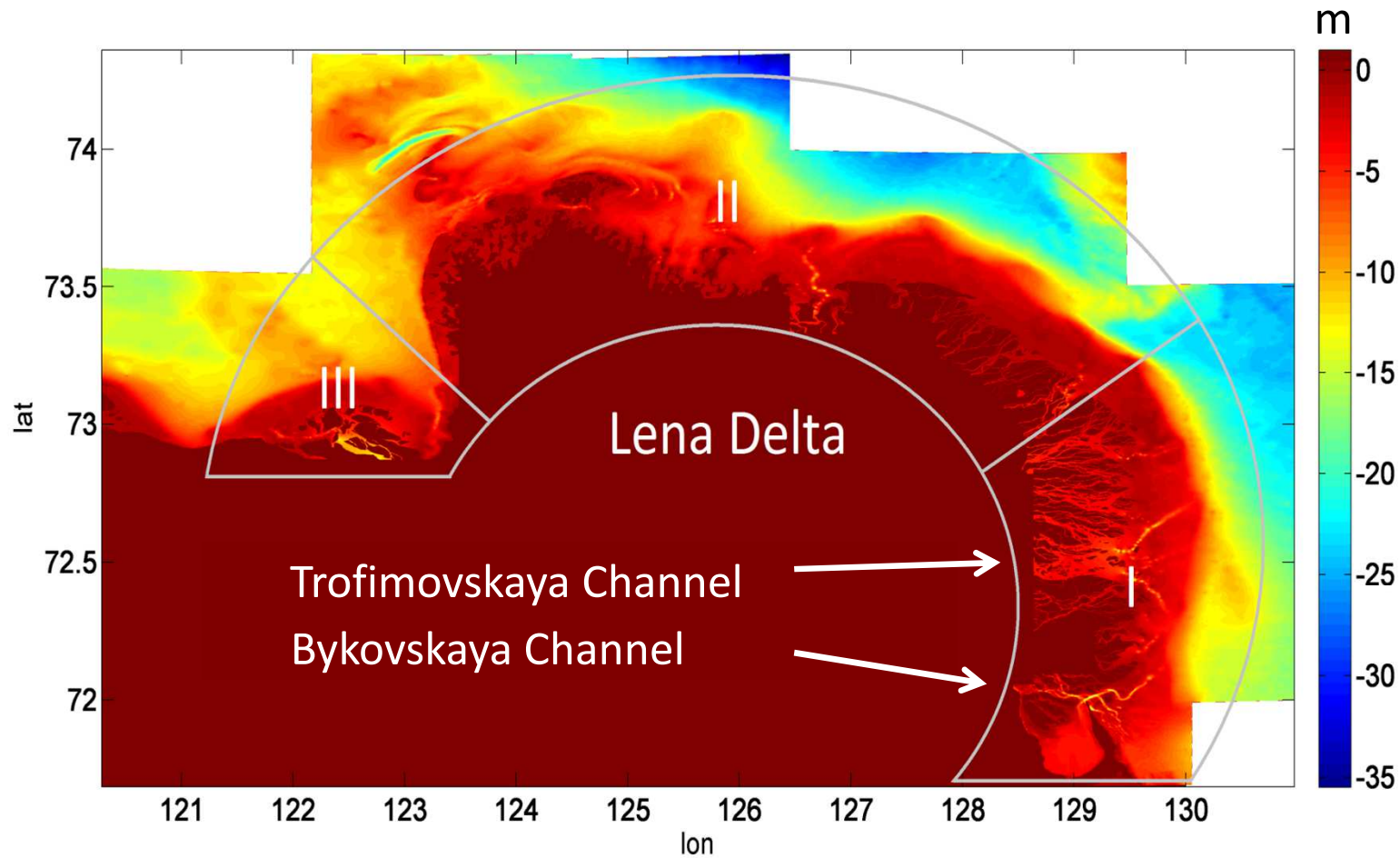


The objects on the map	Distance
Mouth of Ebitiem River – GS Kusur	~5 km
Mouth of Eremeyka River – GS Kusur	~1.5 km
GS Kusur – GS Habarova	~200km
GS Tit-Ary – GS Habarova	~50km

Creating the Lena River hydrological module

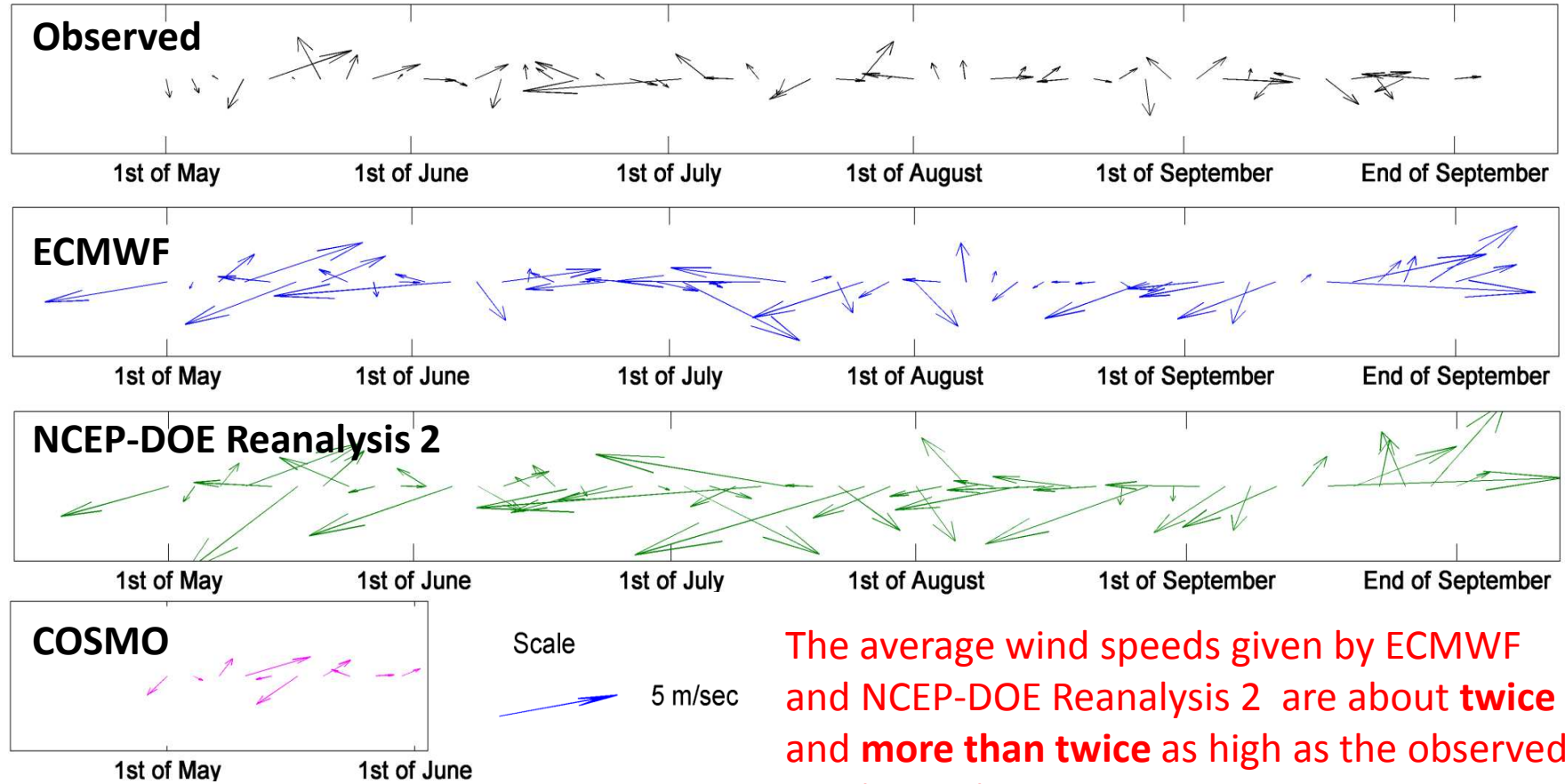


Lena River freshwater plume dynamics



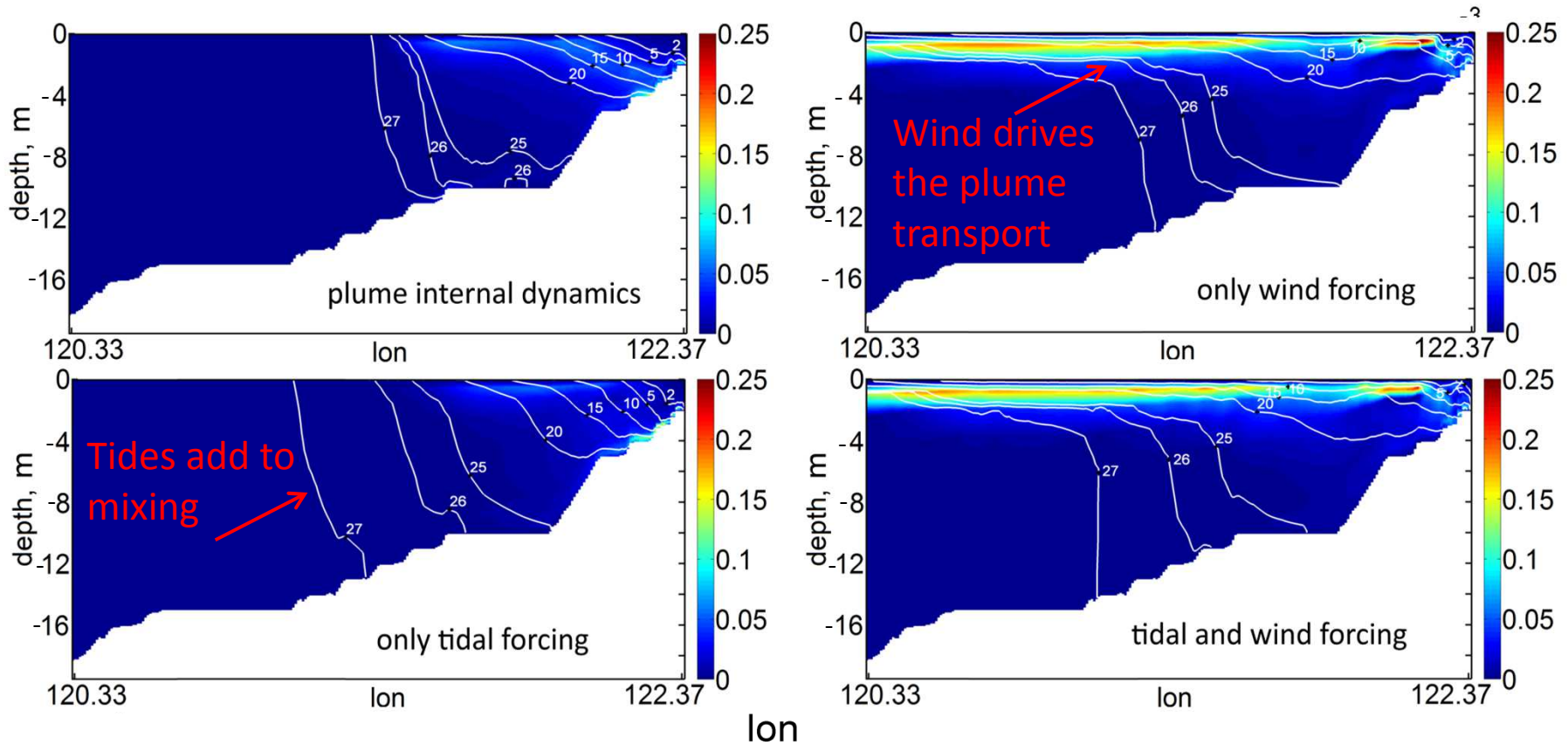
The largest part of the Lena freshwater plume stays in the eastern part of the domain with any type of atmospheric circulation.

Comparison of wind sources



The wind direction and its strength at the Tiksi hydrometeorological station.

Mixing, generated by tides and wind

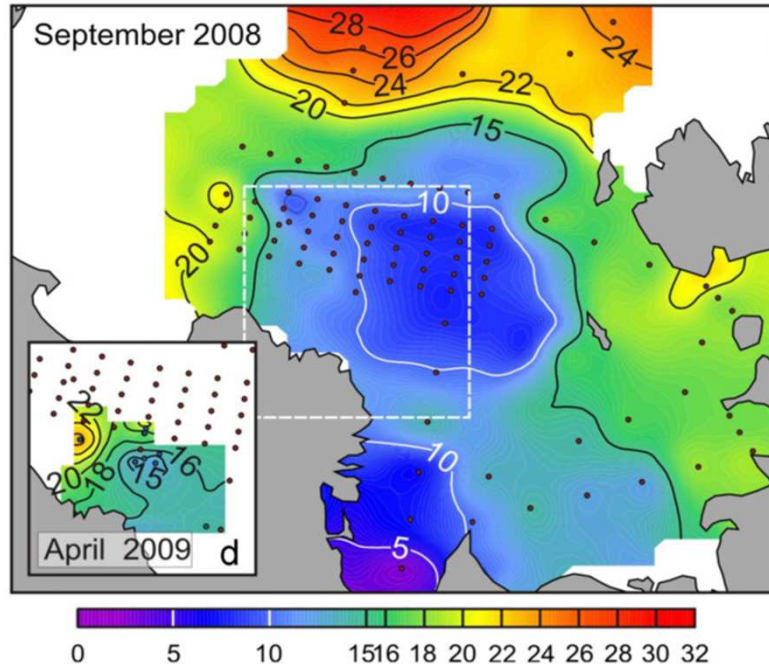


The Brunt-Väisälä frequency (colours) and isohaline lines (white) in section, end of May, 2008; COSMO forcing generated by 12 May at the moment of maximum kinetic energy, [1/s].

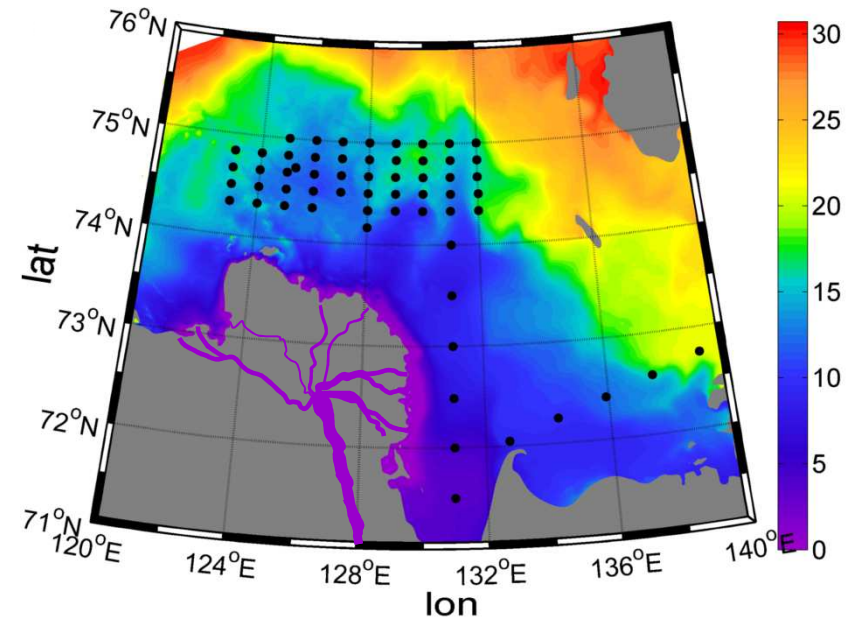
Surface salinity, in practical scale, end of May 2008, COSMO forcing maximum

Wind from COSMO creates a **thin** mixed layer.

Comparison with observations



Observed (Dmitrenko et al., 2010)

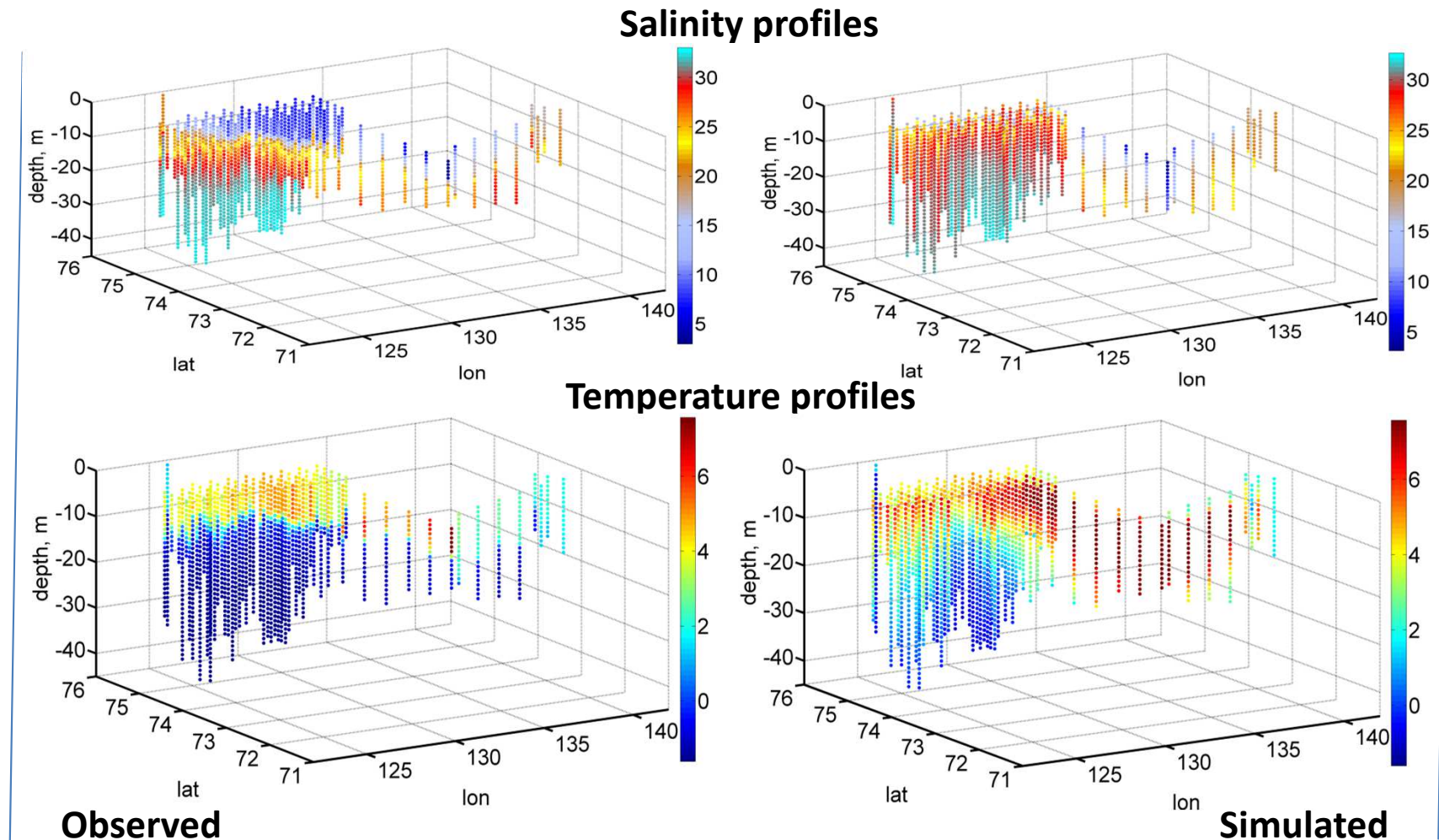


Simulated

Simulated surface salinity, **in practical scale**, driven by ECMWF atmospheric forcing, versus observed surface salinity.

Very good agreement with observed surface salinity map.

Comparison with observations



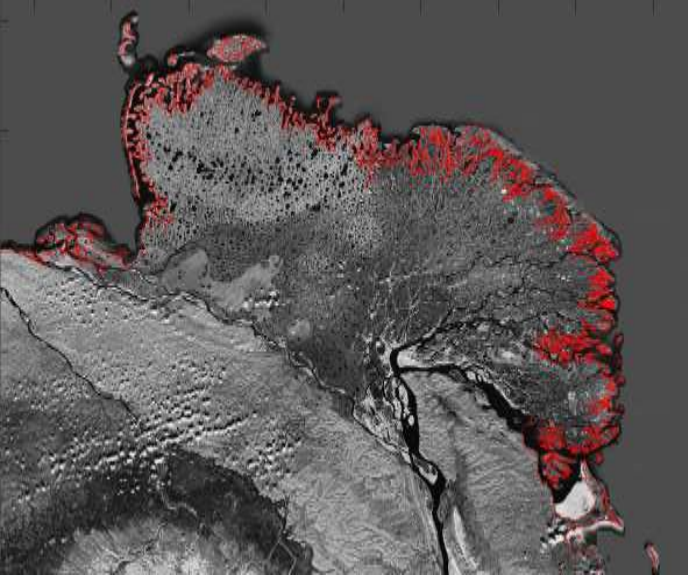
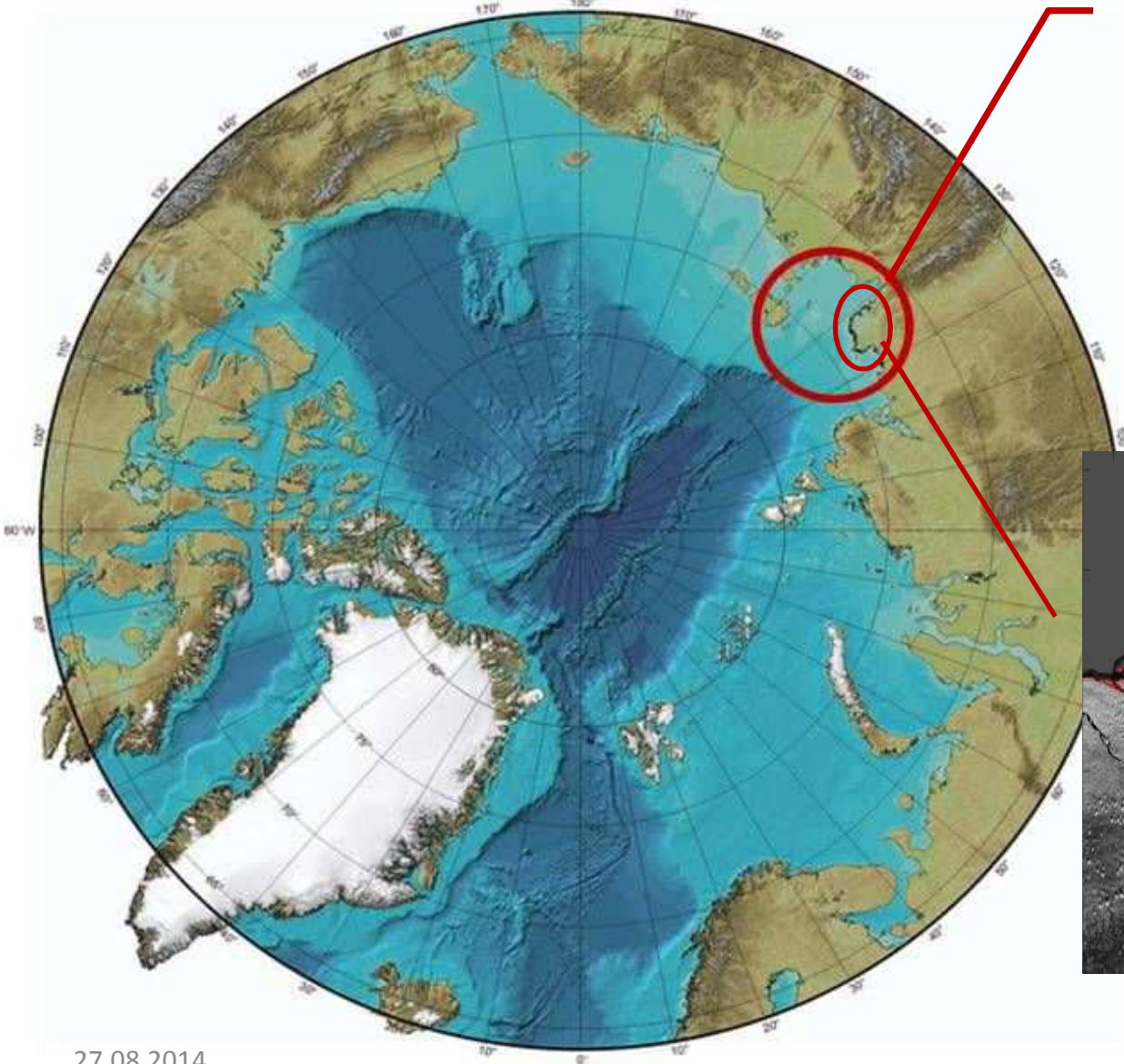
Simulated (right panels) versus observed (left panels) temperature, [$^{\circ}\text{C}$], and salinity, in **practical scale**, for September, 2008.

Summary

- Winds are of primary importance! Northward and westward plume excursions are wind driven, and model skill in simulating them depends on the available wind forcing
- Tides provide additional mixing. Residual circulation associated with tides contributes to the eastward plume propagation along the northern part of the Delta
- East of the Lena Delta the plume dynamics are rather insensitive to the wind and tidal forcing
- Scattered data on the Lena River hydrology have been collected and analyzed

Region of interest

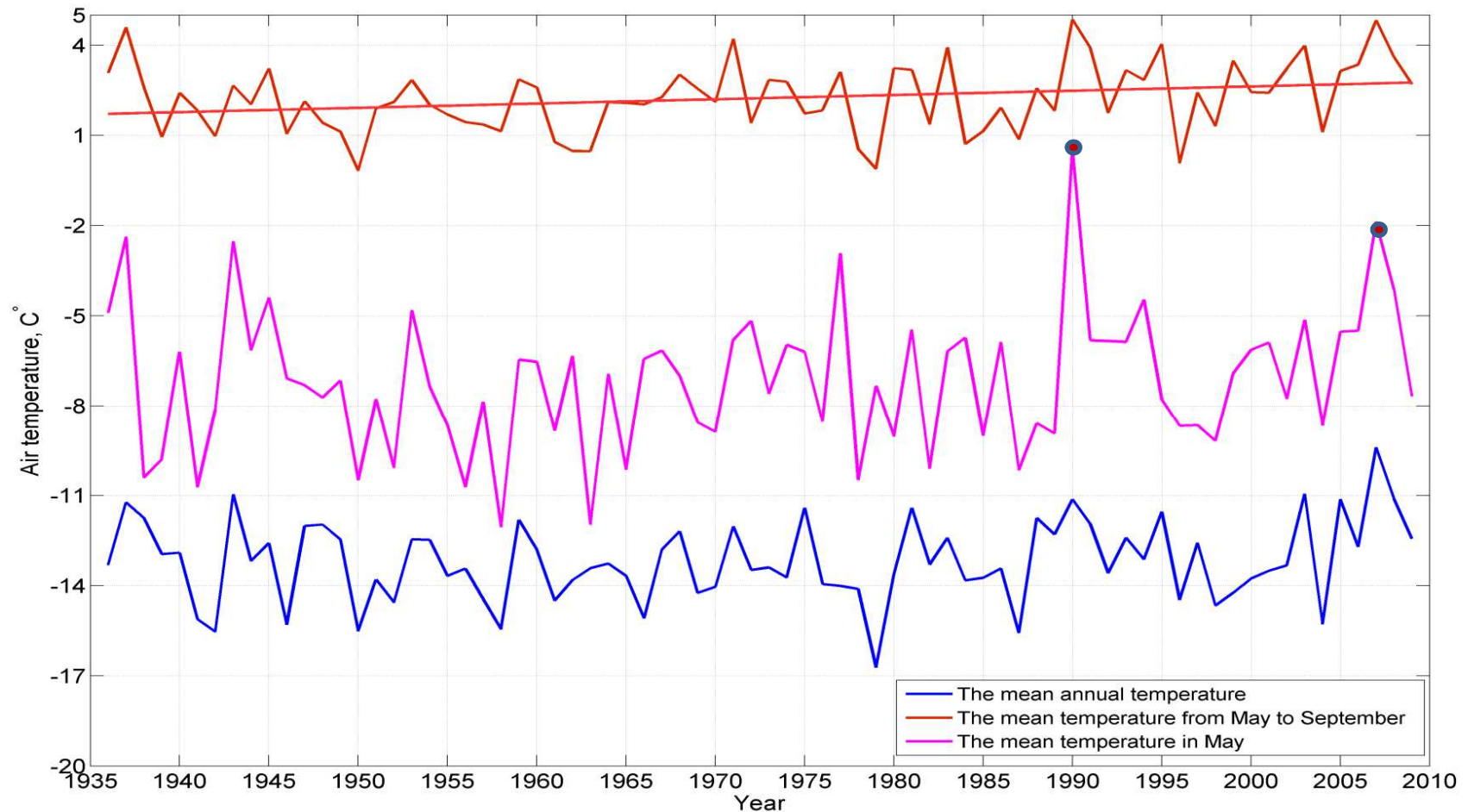
70.7°-76.3°N,
115.9°-141.8°E



Lena Delta

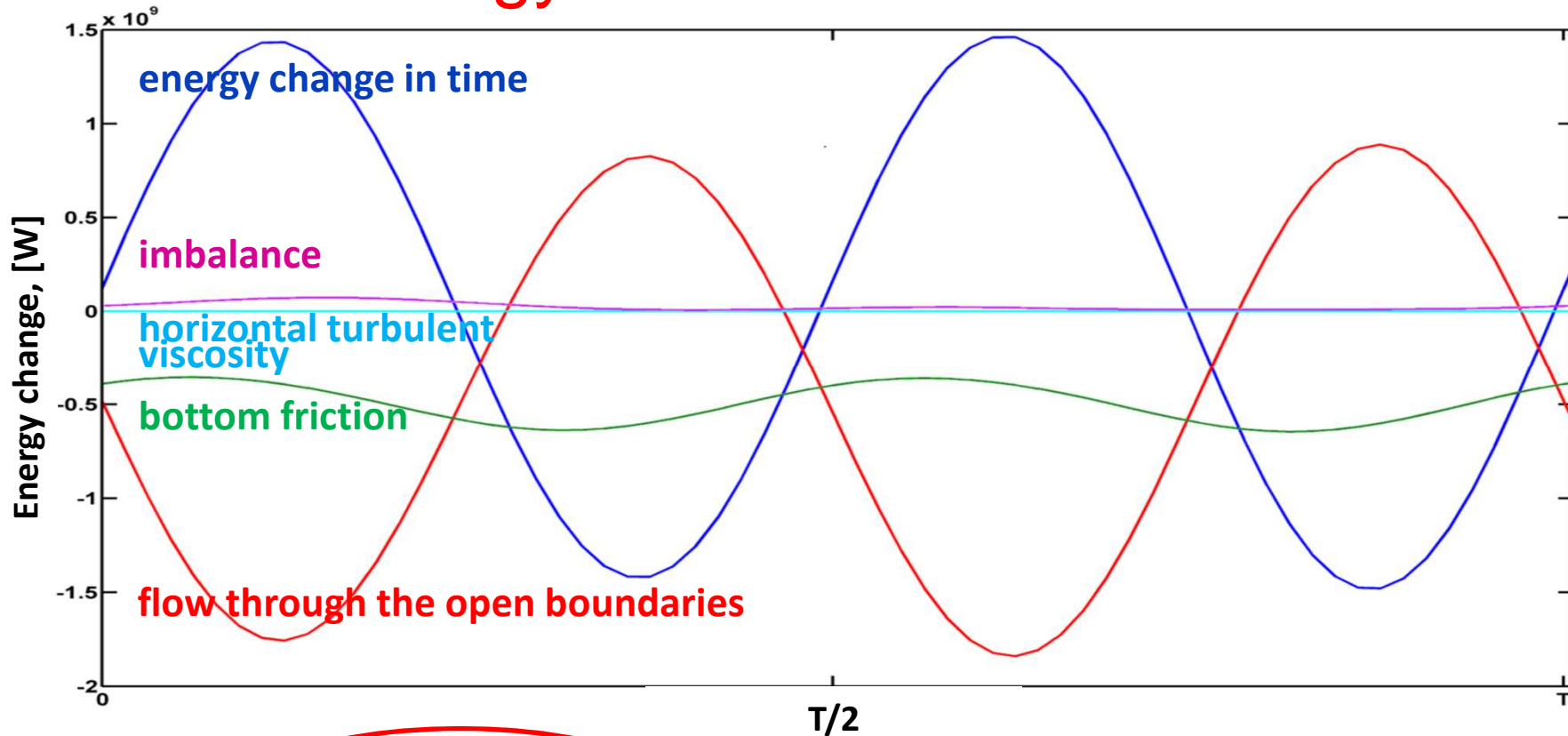
27.08.2014
The picture is taken from International Bathymetric Chart of the Arctic Ocean (IBCAO)

Motivation



The mean surface air temperature from 1936 to 2009, Tiksi Bay. The regression line is shown in red. The theoretical slope of the line is significantly different from 0 with 98% probability.

Energy balance for M2 wave

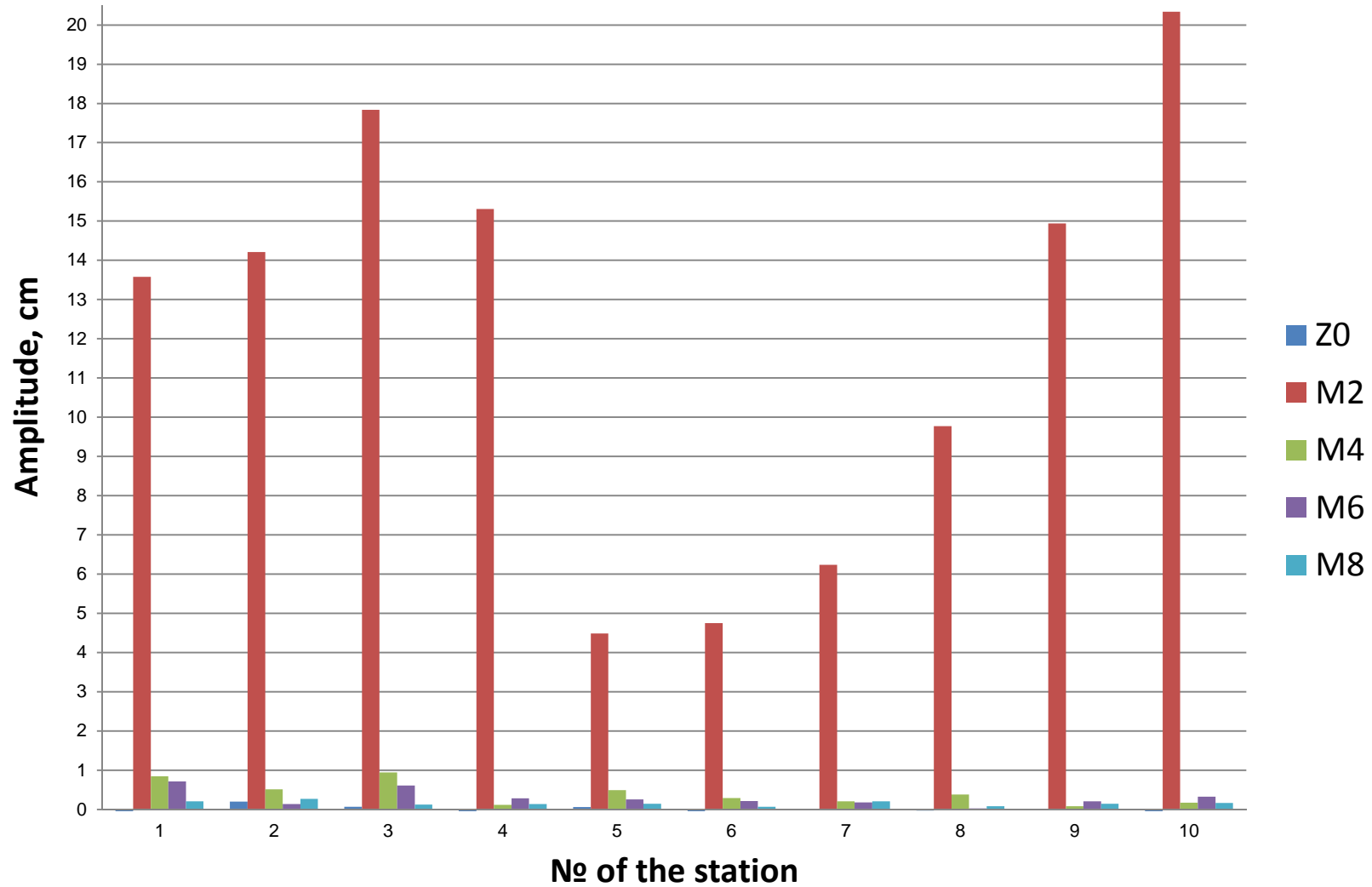


Time, $T=12.42\text{h}$

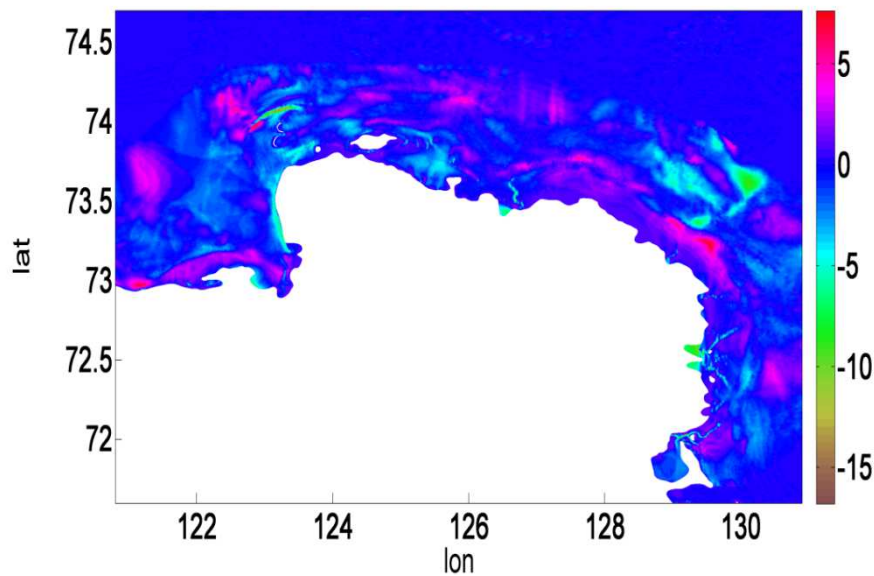
$$\frac{\partial \bar{E}}{\partial t} + \nabla \cdot \left[\rho H \left(g\zeta + \frac{1}{2} |\bar{\mathbf{v}}|^2 \right) \bar{\mathbf{v}} \right] = -\rho r |\bar{\mathbf{v}}|^{3/2} + \rho \bar{\mathbf{v}} \cdot (\nabla \cdot (KH \nabla \bar{\mathbf{v}}))$$

total energy
full depth
surface level
vertically integrated fluid velocity
bottom drag coefficient
eddy viscosity coefficient

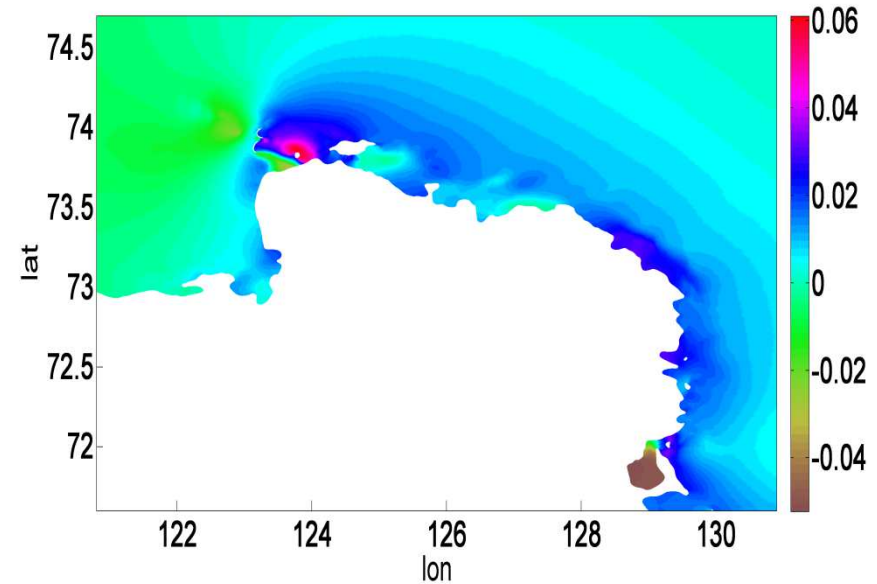
Amplitudes of higher harmonics at all coastal stations where nonlinearity can be expected to be noticeable



Sensitivity to bathymetry



a)

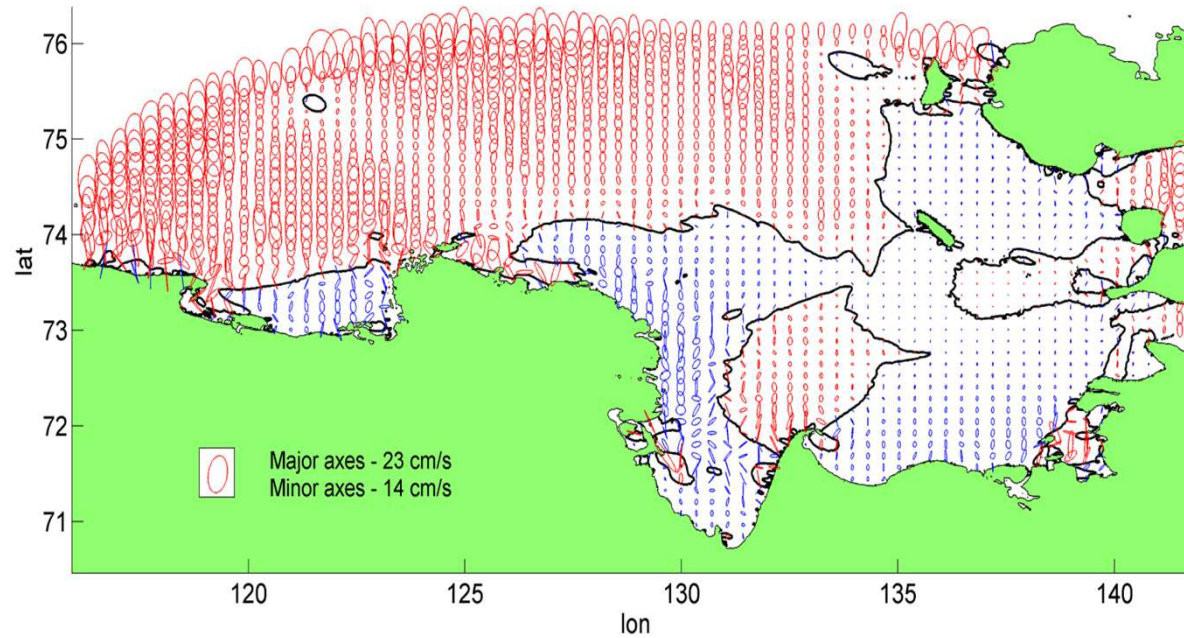


b)

a) The difference between GEBCO bathymetry and additional bathymetric data from the digitized Soviet map, [m].

b) The differences between amplitudes of the M2 wave in simulations based on GEBCO and modified bathymetry, [m].

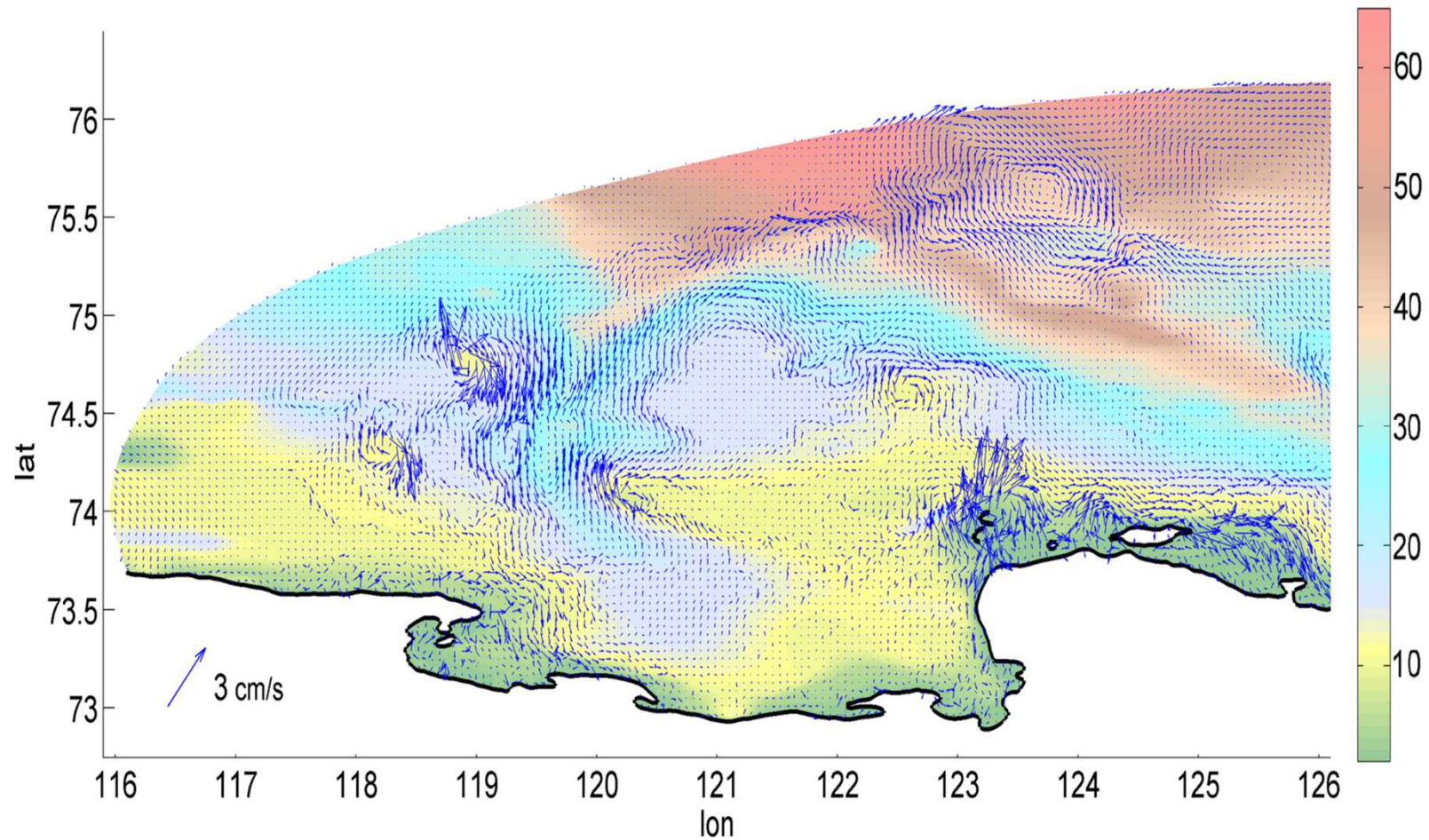
Tidal ellipses



Ellipses of barotropic velocities for the M2 tide, red ellipses have CW rotation, blue ellipses have CCW rotation.

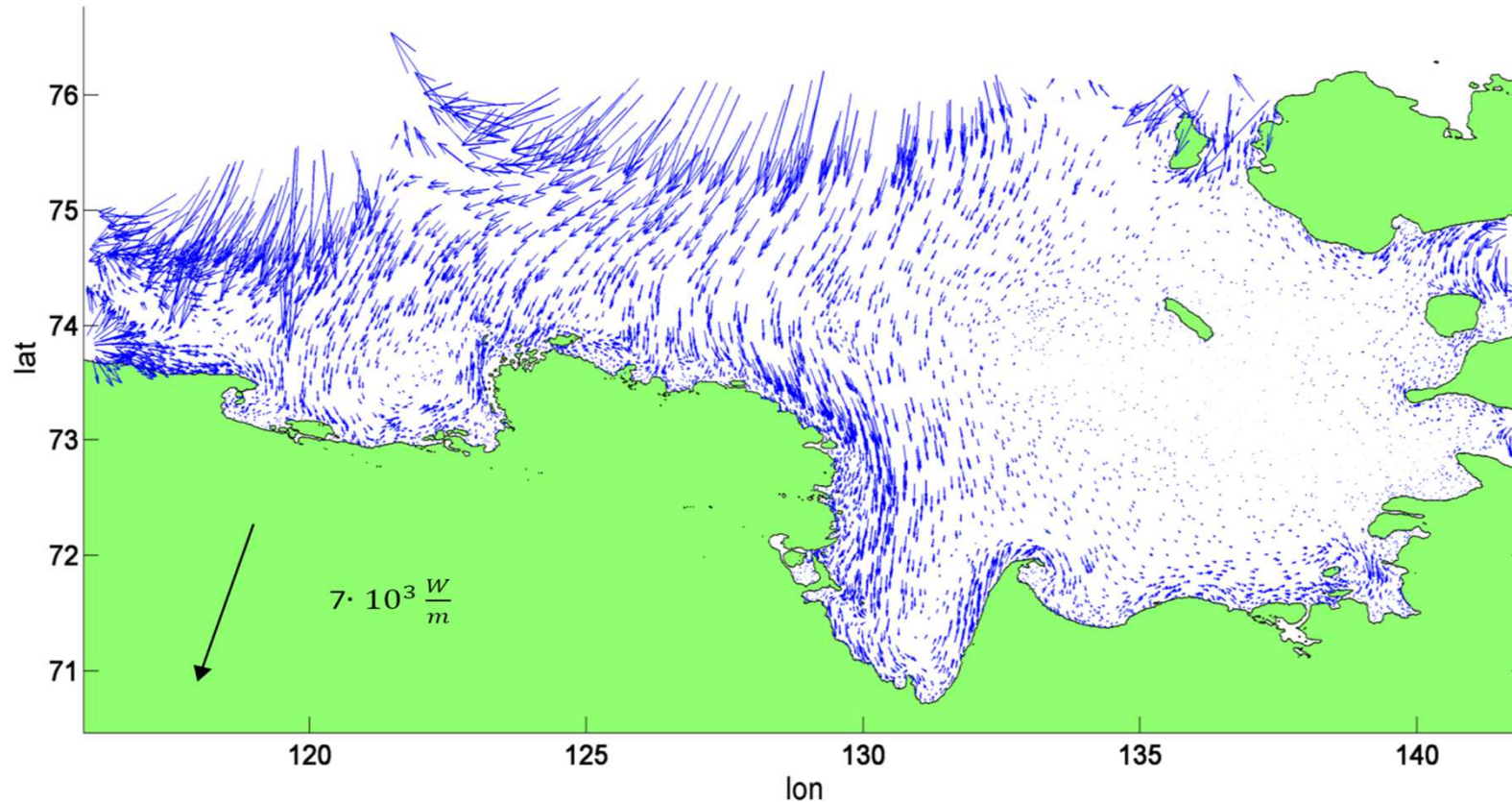
Comparison of ellipse parameters with AWI moorings data (5 stations) for M2(S2) waves				
Solution	AOTIM5	TPX07.1	TPX06.2	Model with OOBBC
Ellipse parameters				
Error_major axes, [cm/s]	6.3(4.1)	4.7(2.7)	2.9(3.9)	1.4(1.5)
Error_minor axes, [cm/s]	1.2(1.3)	2.3(0.9)	2.8(3.3)	3.2(2)

The residual circulation for M2 wave



Residual circulation, [**cm/s**], superimposed on bathymetry map, [**m**], for the western part of the domain.

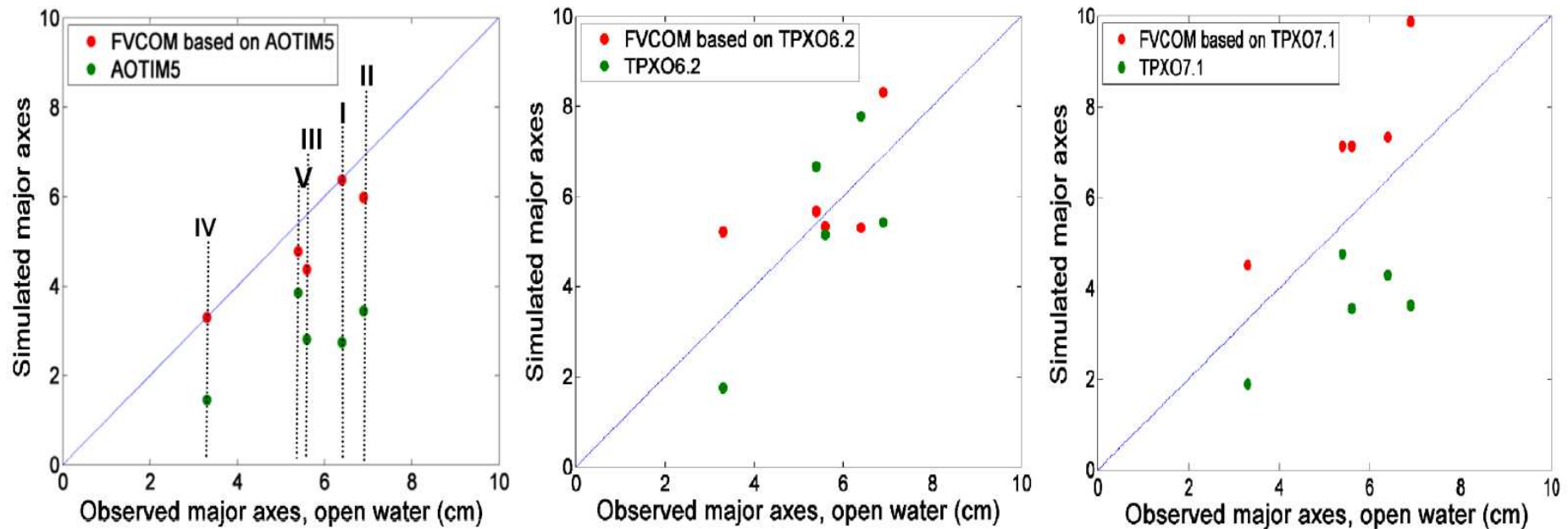
Energy fluxes for M2 wave



$$(E_\lambda, E_\theta) = \frac{1}{T} \int_0^T \rho H \left(g\xi + \frac{1}{2} |\bar{\mathbf{v}}|^2 \right) \bar{\mathbf{v}} dt$$

E_λ, E_θ – zonal and meridional components of the tidal energy flux vector, T is the tidal period.

Comparison of major axes



Comparison of major axes in simulations based on the open boundary conditions from different inverse models and predicted directly by these models with observational data.

$$Error = \frac{1}{N} \sum_{i=1}^N \left(\left(1 + \left(\frac{A_S(i)}{A_O(i)} \right)^2 - 2 \cdot \cos \left(\frac{P_S(i) - P_O(i)}{2} \right) \cdot \frac{A_S(i)}{A_O(i)} \right)^{\frac{1}{2}} \right)$$

$$\frac{\partial \bar{E}}{\partial t} + \nabla \cdot \left[\rho H \left(g \zeta + \frac{1}{2} |\bar{\mathbf{v}}|^2 \right) \bar{\mathbf{v}} \right] = -\rho r |\bar{\mathbf{v}}|^{3/2} + \rho \bar{\mathbf{v}} \cdot (\nabla \cdot (KH \nabla \bar{\mathbf{v}}))$$

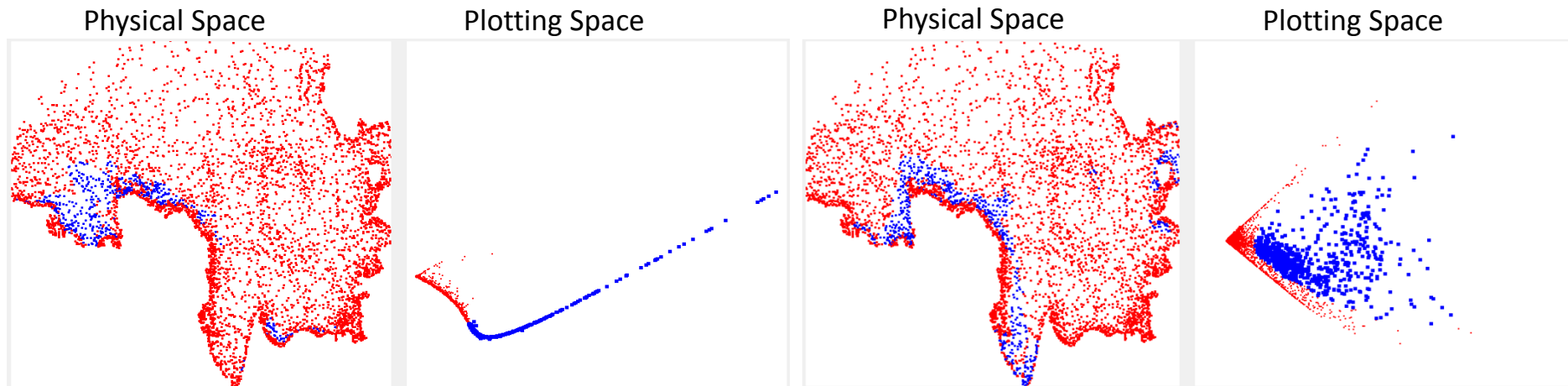
Annotations for the equation above:

- $\frac{\partial \bar{E}}{\partial t}$: total energy per unit area
- ρ : density
- H : full depth
- ζ : surface level
- $g \zeta + \frac{1}{2} |\bar{\mathbf{v}}|^2$: acceleration due to gravity
- $\bar{\mathbf{v}}$: vertically integrated fluid velocity
- r : bottom drag coefficient
- KH : eddy viscosity coefficient

- Our model reproduces semidiurnal tidal waves in the Laptev Sea shelf region
- A procedure for the construction of optimal open boundary conditions for tidal elevation for M2 and S2 waves has been proposed
- Simulated tidal maps show an improved agreement with observations
- We analyzed energy balance, residual circulation and energy fluxes in the region
- We explored sensitivity to the bathymetry

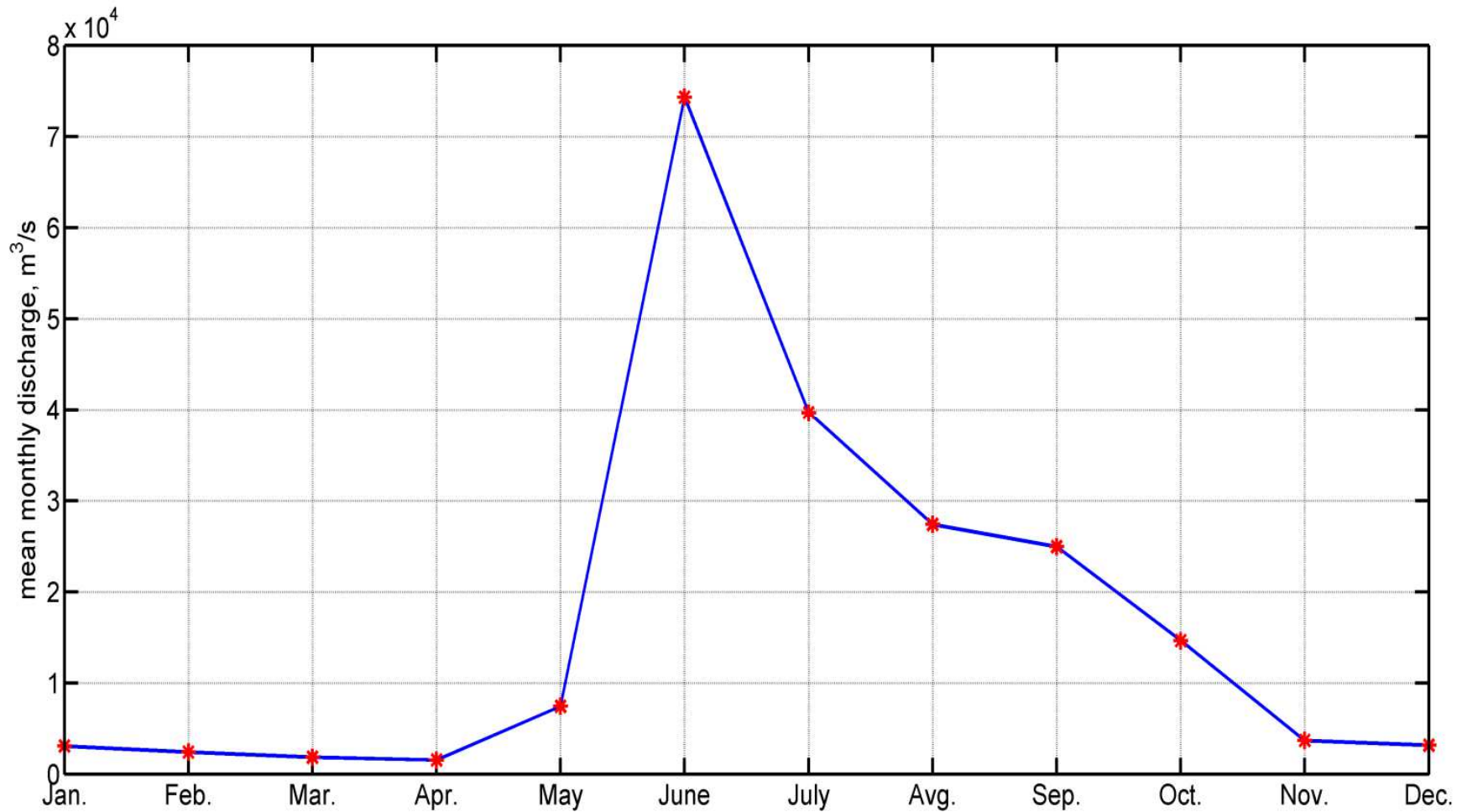
MDS projection

Impact of different factors (tides and wind) on the Lena River freshwater plume spreading in the region



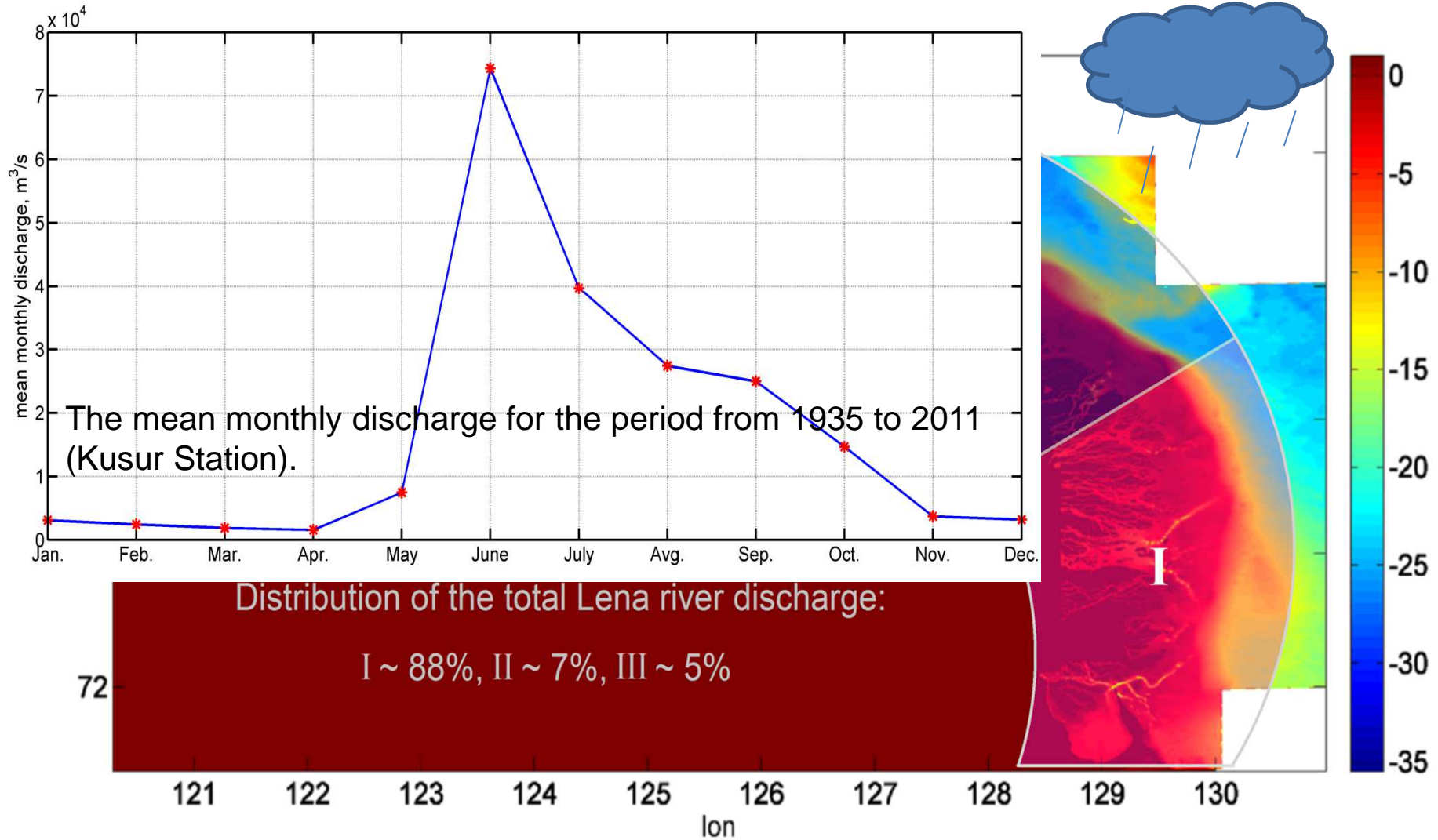
MDS projection method for Brunt–Väisälä frequency in simulations without tides (left panel) and without wind forcing (right panel)

Lena River discharge seasonal variability



The mean monthly discharge for the period from 1935 to 2011 (Kusur Station).

Creating the Lena River hydrological module



Temperature anomaly and its description

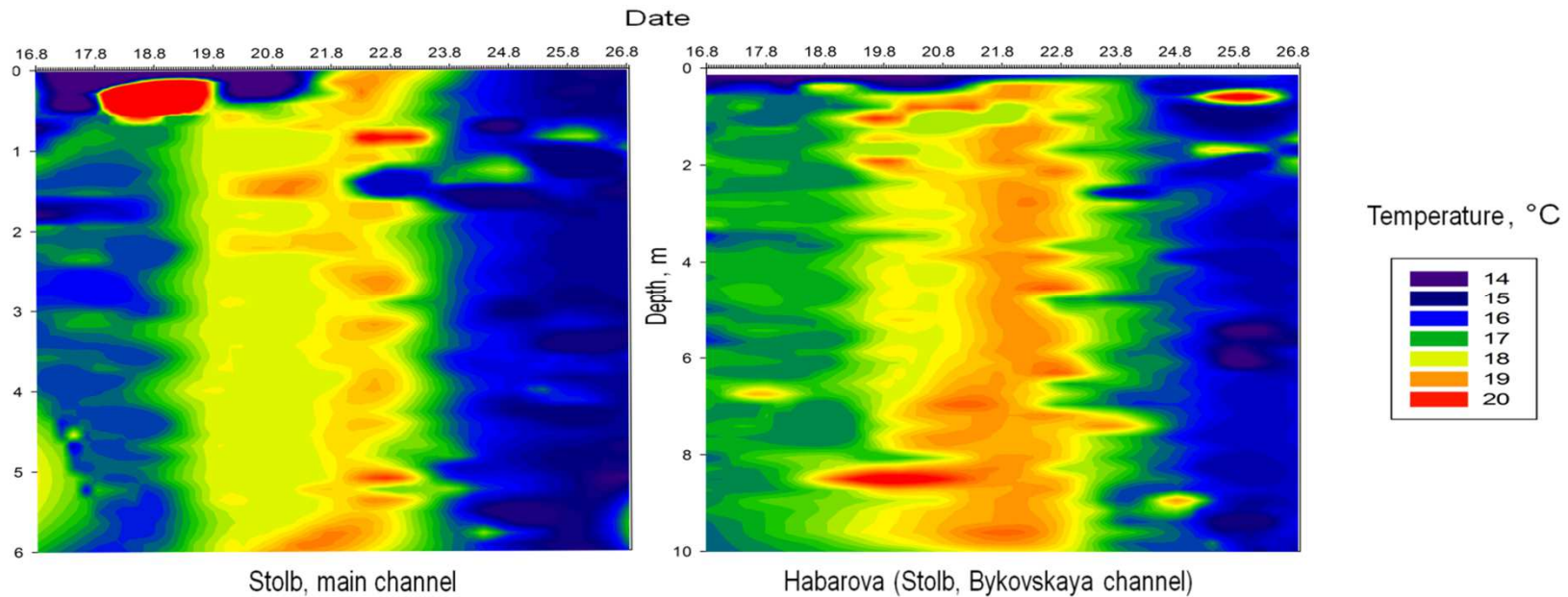


Fig. 7. Stream temperature profiles and mean surface air temperatures on a corresponding date. The water temperature measurements were carried out at midstream, at 10.30 a.m., in the same time every day. The surface air temperature was measured twice per day, at 8 a.m. and 8 p.m., and then averaged. Depth is counted down from the free surface.

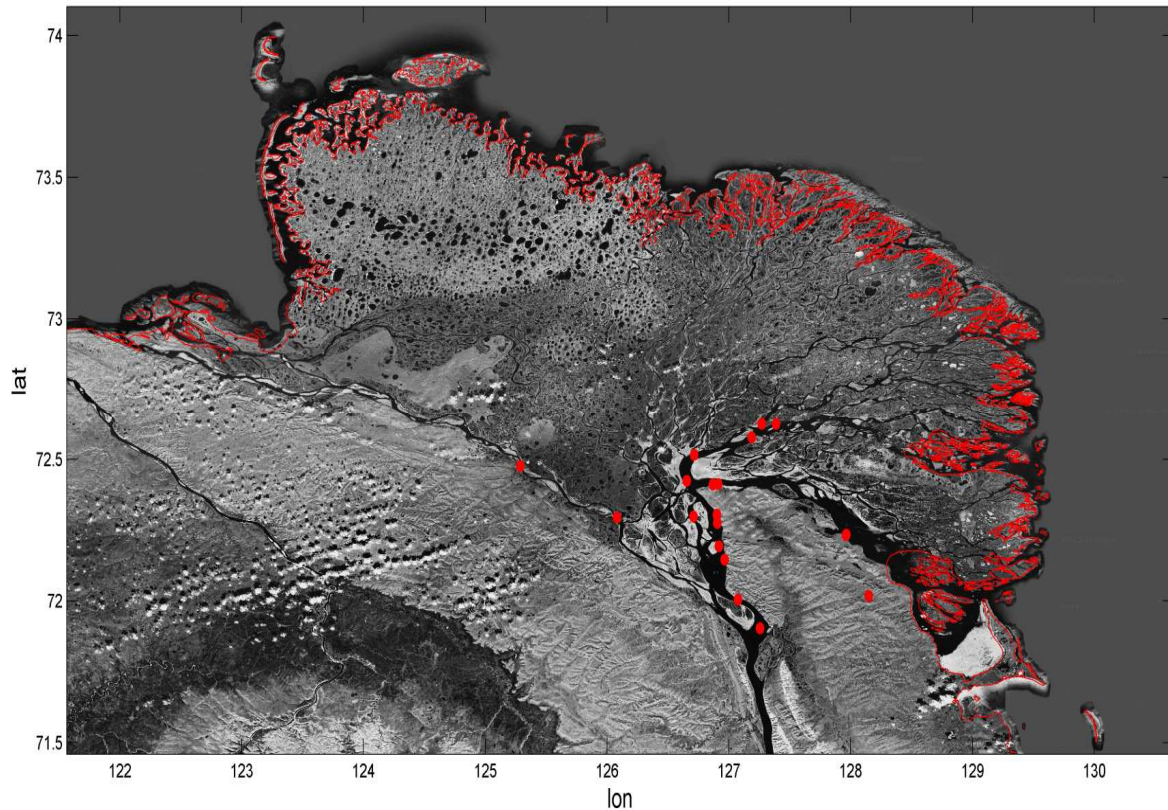
Daily mean air temperature in August, 2011													
Date Station	16.8	17.8	18.8	19.8	20.8	21.8	22.8	23.8	24.8	25.8	26.8	16.8	17.8
Stolb, main channel	8	6.4	7.8	11.1	13.1	12.2	8.2	4.9	4.2	No data	No data	8	6.4
Habarova (Stolb, Bykovskaya)	8.1	6.5	6.2	7.8	13.5	11.9	7.5	4.9	3.6	3.5	4.8	8.1	6.5

Daily water temperature prediction

$$T_w = \mu + \frac{\alpha - \mu}{1 + e^{\gamma(\beta - T_a)'}}$$

where , T_w – water temperature,
 T_a – air temperature,
 μ – lowest water temperature,
 α – highest water temperature,
 γ – function of the steepest slope
(inflection point) of the T_w function
(when plotted against T_a),
 β – air temperature at the
inflection point.

Nash-Sutcliffe coefficient of
efficiency equals to **0.73 for weekly
scale** and on average **0.3 (varies
from 0.6 to 0.1 from June to August)**
for monthly scales.



The stations with known temperature profiles

Nash–Sutcliffe model efficiency coefficient

$$E = 1 - \frac{\sum_{t=1}^T (Q_o^t - Q_m^t)^2}{\sum_{t=1}^T (Q_o^t - \overline{Q_o})^2}$$

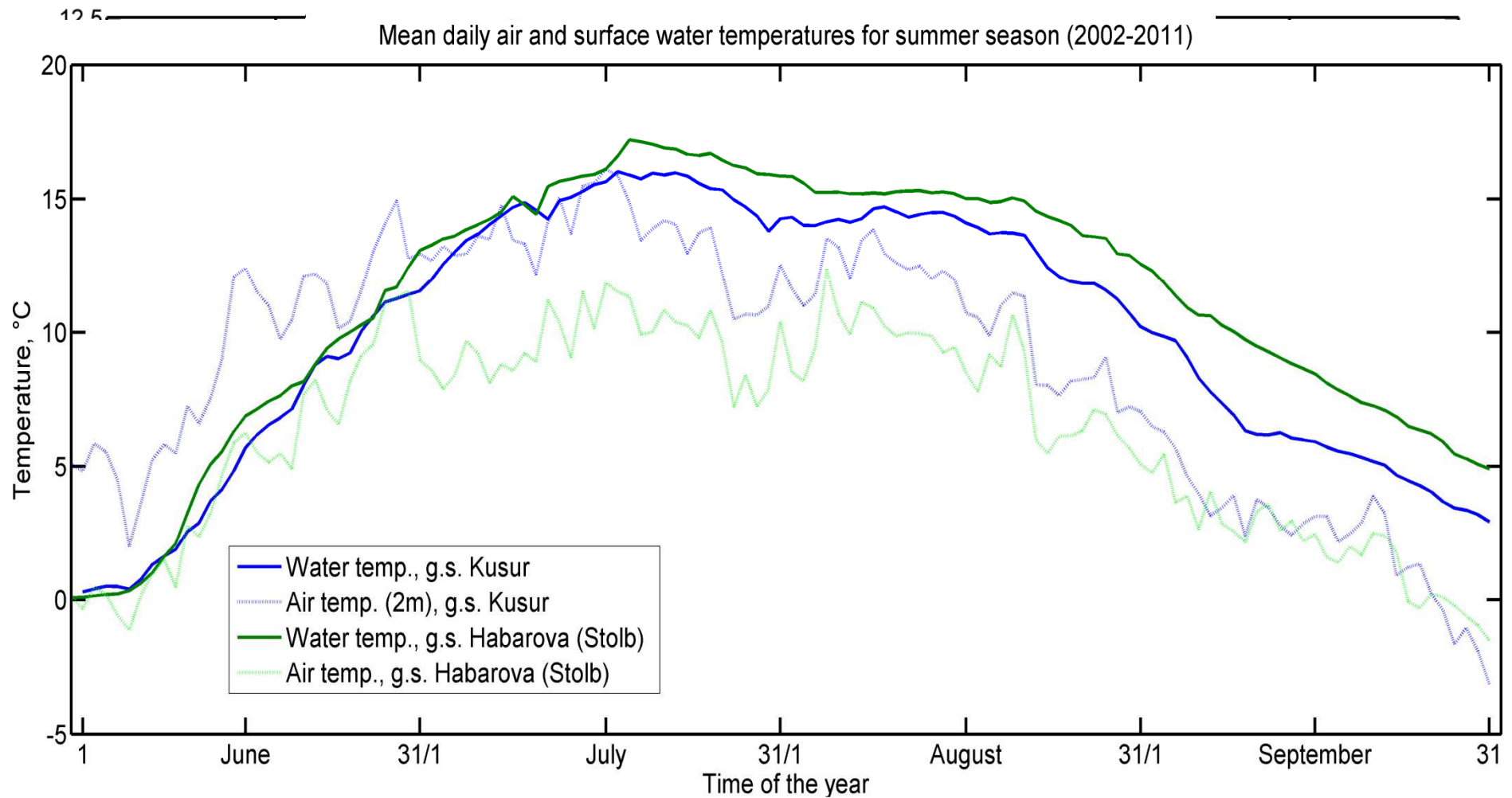
where Q_o is the mean of observed temperatures/discharges,

Q_m is modeled temp./discharge,

Q_o^t is observed temp./discharge at time t .

Nash–Sutcliffe efficiencies can range from $-\infty$ to 1.

Kusur-Habarova (Stolb) surface water temperature anomaly



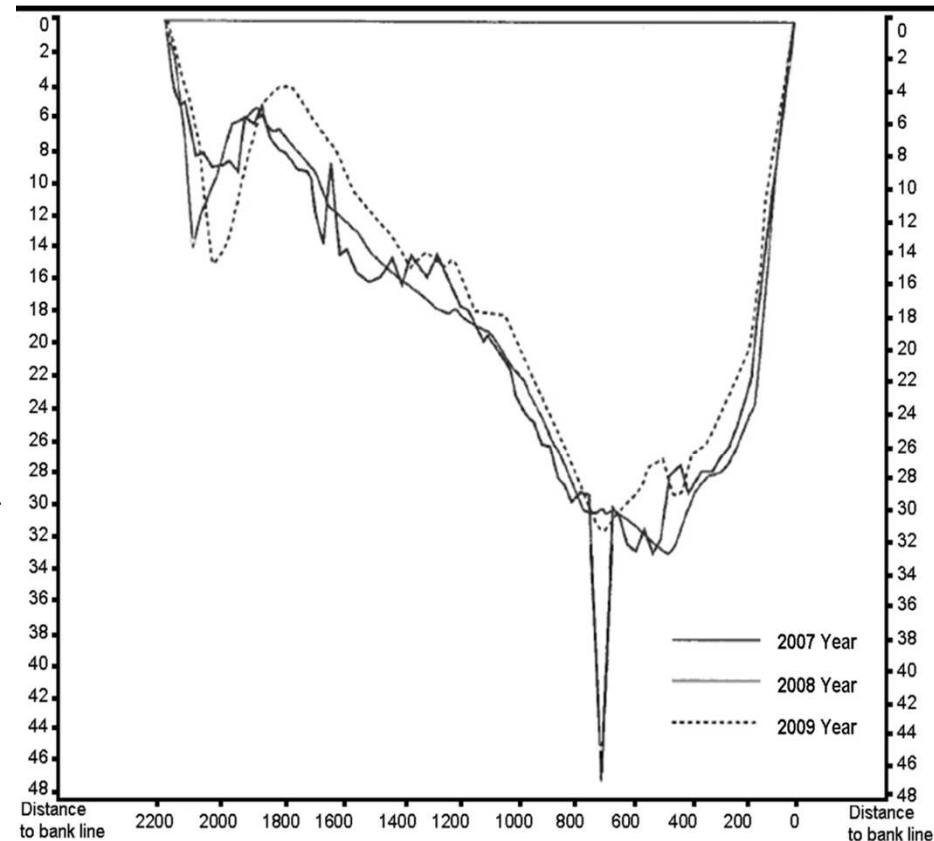
Water temperature anomaly and its description

Anomaly can be explained by at least 60% by cold right bank current

Significant trends exist only for August at Kusur and for June at Habarova stations indicating the temperature increase by ~ 1.3 °C for both stations since the beginning of observations.

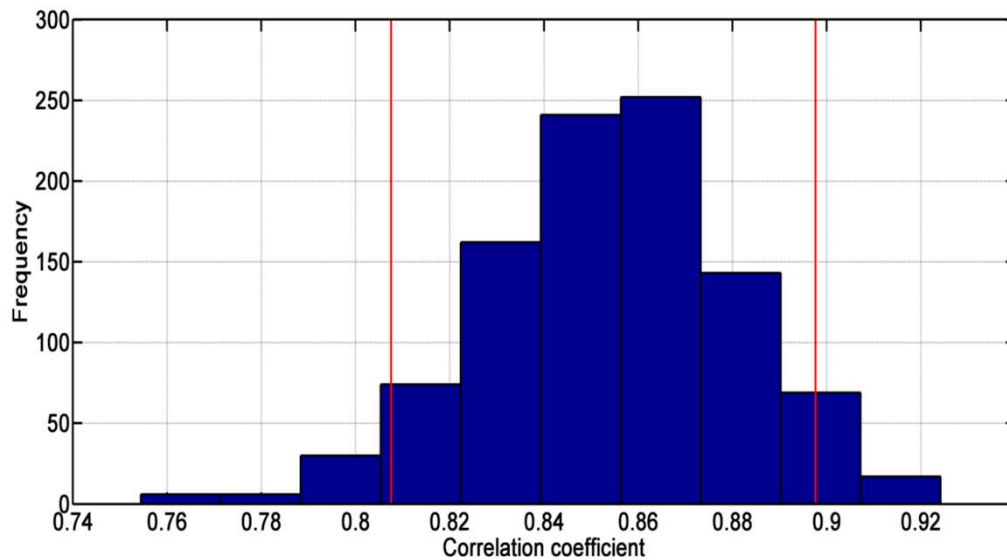
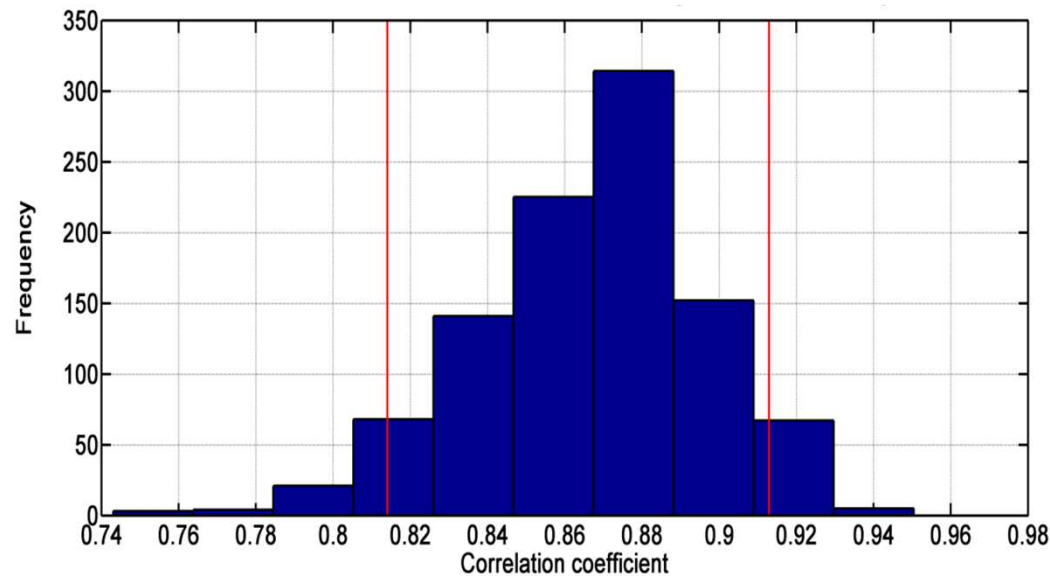
There are indications in favor of unaccounted source of heat from the river bed in the area of delta head.

One of the most difficult issues is the morphological structure of the underflow, which can be responsible for releasing the heat stored earlier in the season.



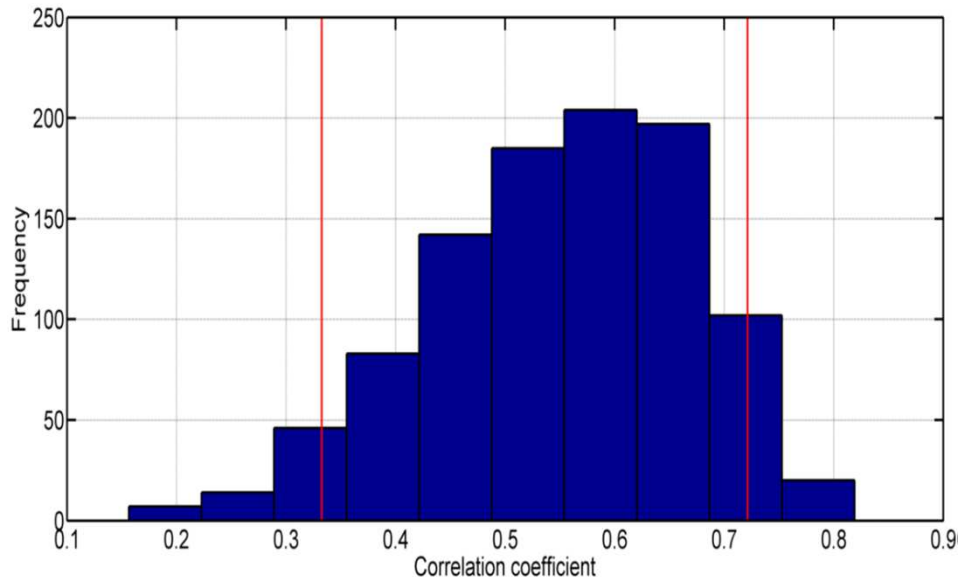
The Lena River bed profile, area of GS Stolb, main channel, August [m]. The picture is taken from Bolshiyarov et al., 2013.

Water temperature anomaly and its description



The correlation between mean monthly surface temperatures measured at GS Kusur and Eremeyka. The lines confine 95% confidence interval. Since the lower end of our confidence interval is above zero, we conclude that our correlation is significant at the $p < 0.01$ level (two-tailed). The 148 data points (the data set contains monthly mean values for open water season from 1974 to 2010) are resampled to create 1000 different data sets, and the correlation between the two variables is computed for each data set. The histogram shows the variation of the correlation coefficient across all the bootstrap samples.

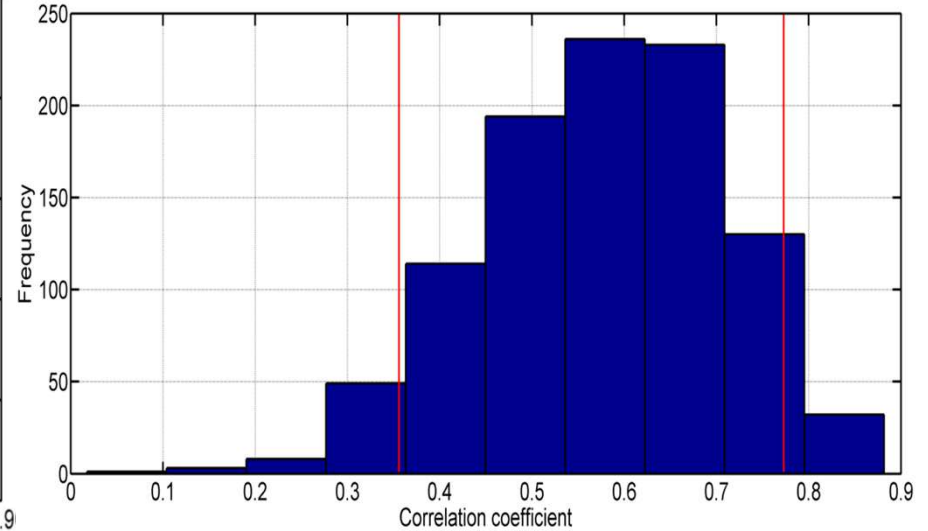
The correlation between surface temperatures measured at GS Habarova and Eremeyka. The 148 data points (the data set contains monthly mean values for open water season from 1974 to 2010) are resampled to create 1000 different data sets. The other details are the same as for upper picture.



The correlation between the normalized surface water temperature at GS Eremeyka (x_1) and amplitude of anomaly (x_2). The 148 data points (the data set uses monthly mean values for open water season from 1974 to 2010) are resampled to create 1000 different data sets.

$$x_1 = \frac{TW_{Erem}}{TW_{Hab}}$$

$$x_2 = -(TW_{Hab} - TW_{Kus}) / TW_{Hab}$$

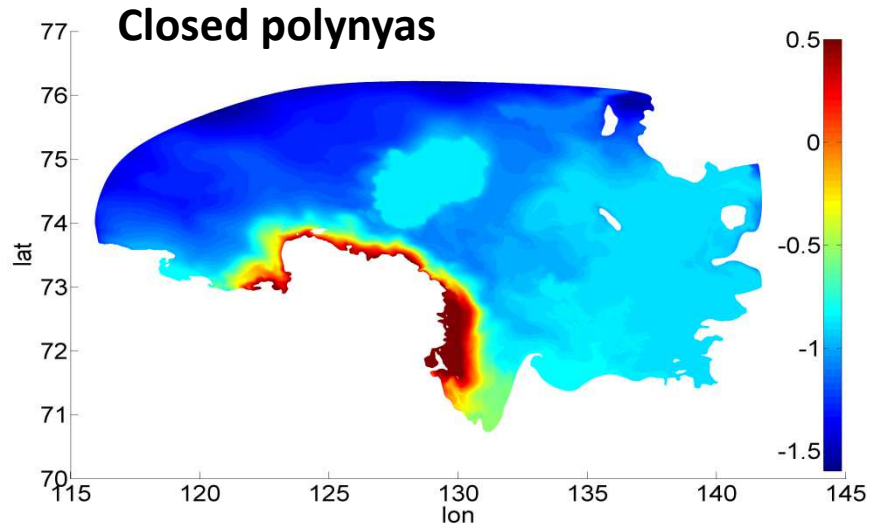


The correlation between times at GS Kusur and Habarova when the surface water temperature reaches the maximum. 60 data points (the data set contains times for each year from 1951 to 2010) are resampled to create 1000 different data sets.

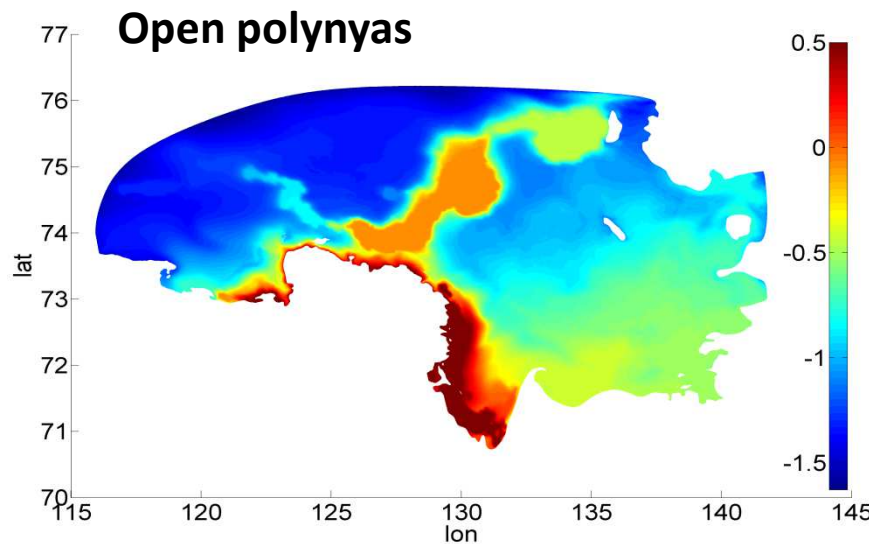
$$\frac{TW_{Erem}}{TW_{Hab}} \frac{TW_{Kus}}{TW_{Hab}}$$

are the water temperature measured at GS Eremeyka, Habarova (which is representative) and Kusur

Study of the effects of forcing modified with the presence of polynyas

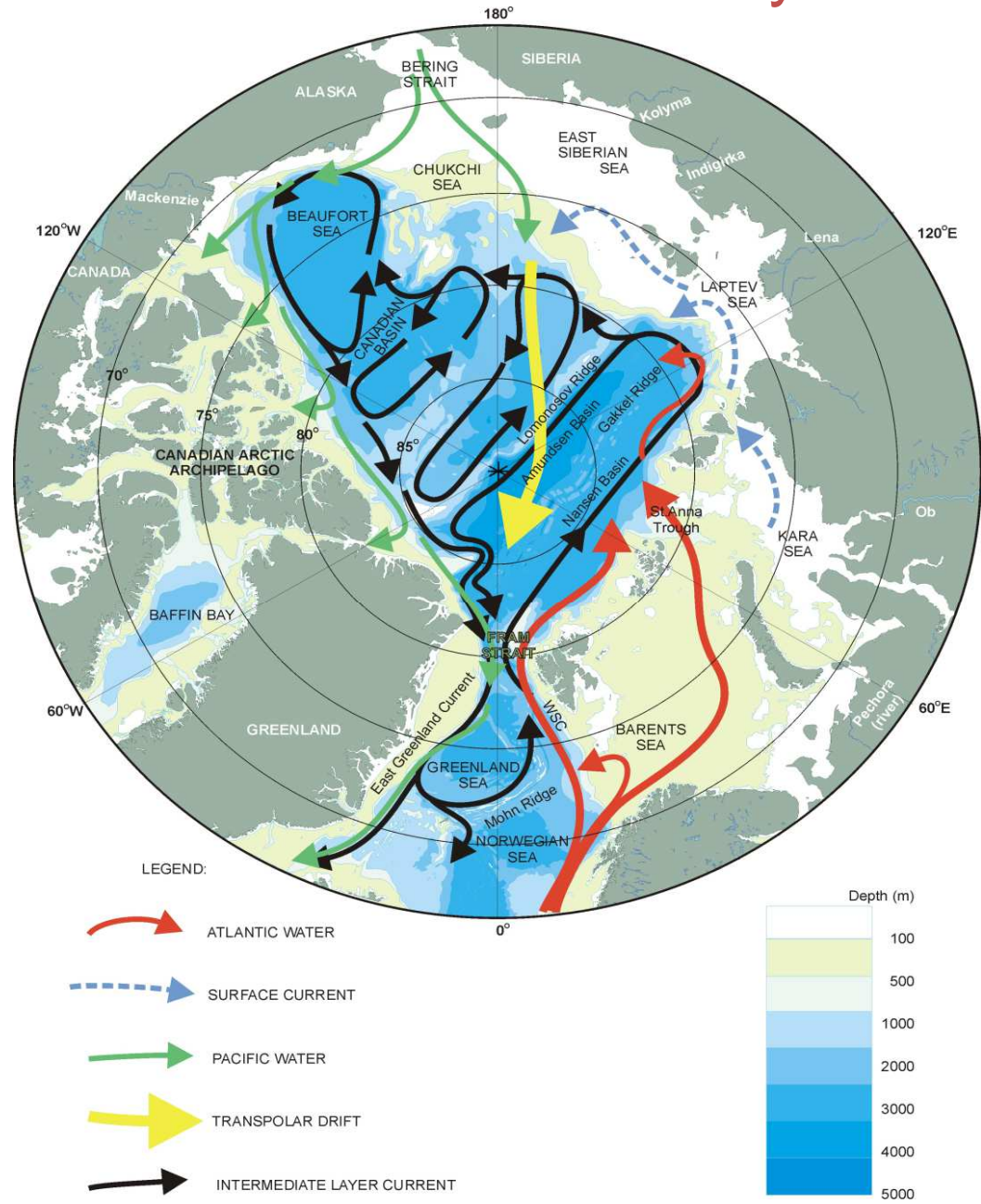


The surface temperature fields [$^{\circ}\text{C}$], at the end of May, 2008; COSMO forcing

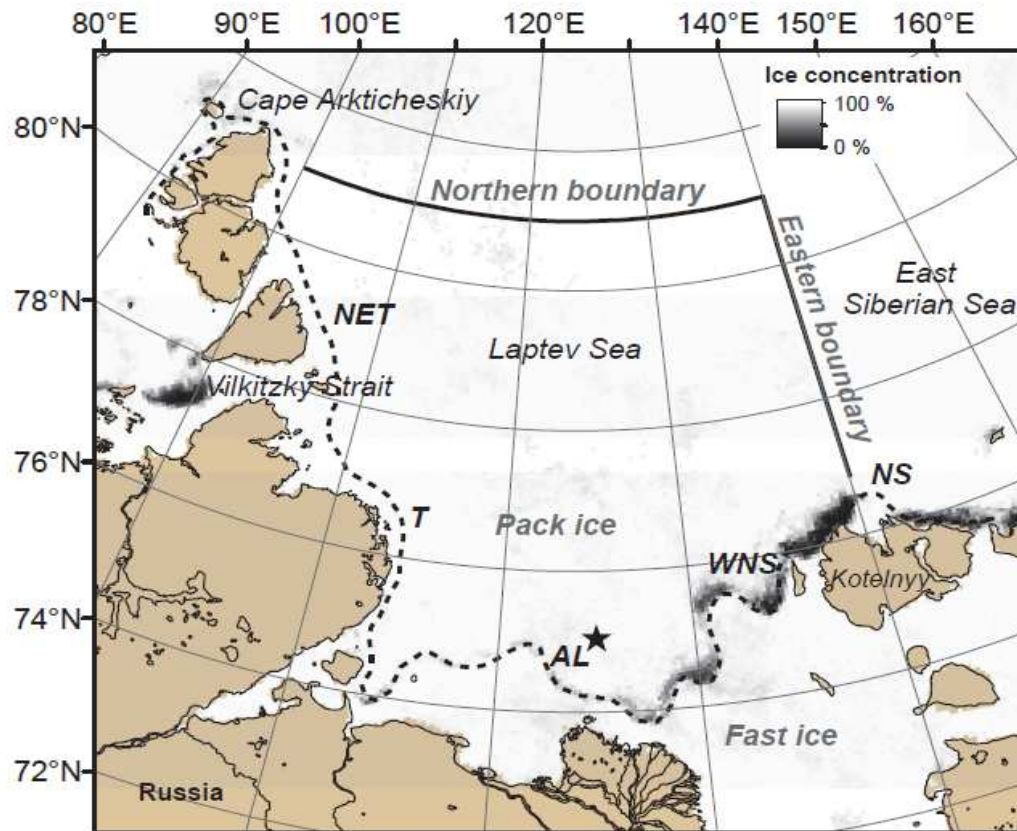


Change in the structure of heat fluxes influences the temperature pattern in the whole mixing layer

Pathways of Atlantic water and Entry of Pacific water



Polynyas and borders

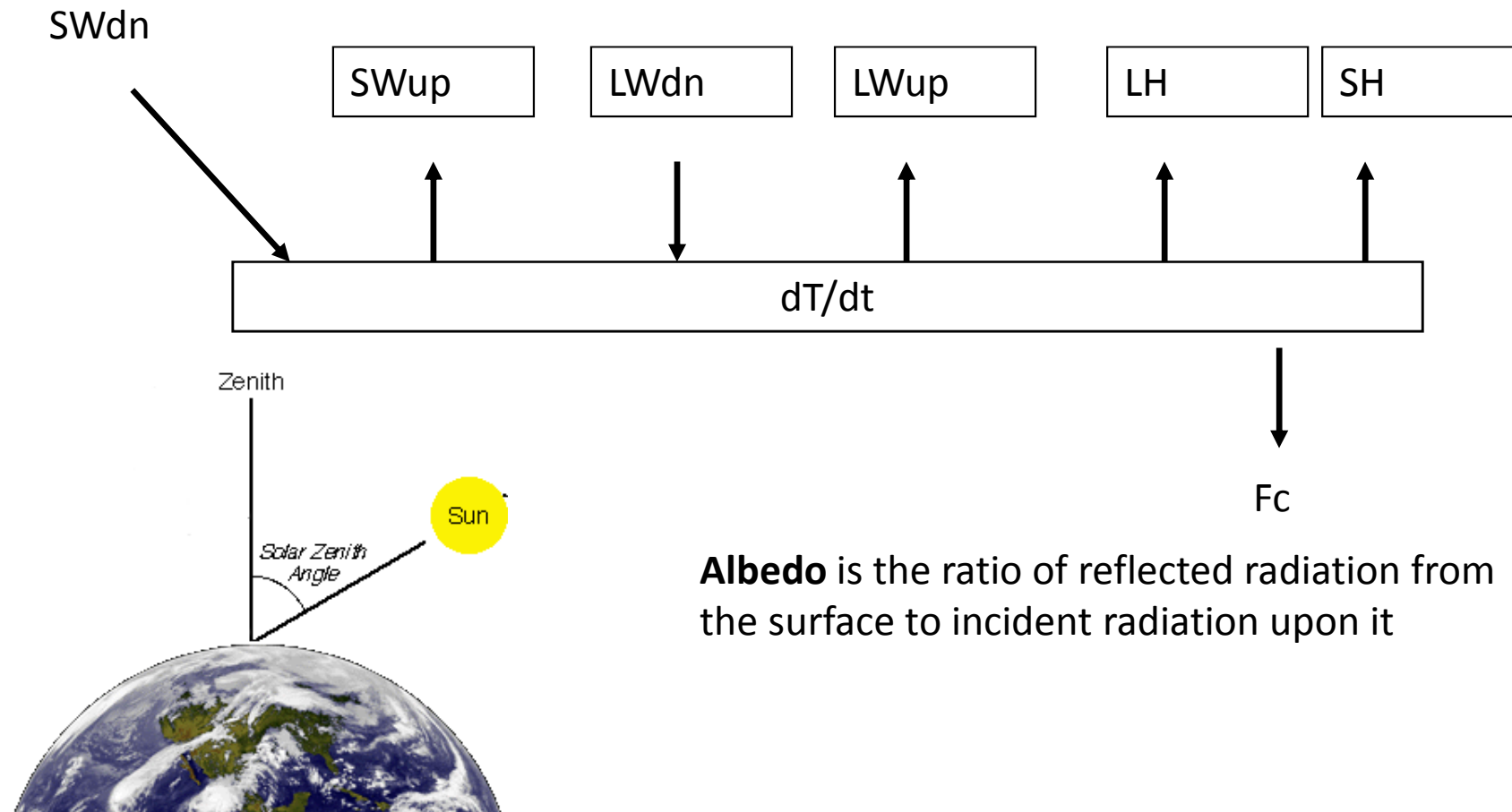


The geographical location of the Laptev Sea and the northern and eastern boundaries (solid black lines). The dashed line represents the mean fast ice edge location. Between pack ice and fast ice edge, flaw polynyas are formed: The New Siberian polynya (NS), the Western New Siberian polynya (WNS), the Anabar-Lena polynya (AL), the Taymyr polynya and the North-Eastern Taymyr (NET) polynya.

Color coding corresponds to the sea ice concentration as obtained from Advanced Microwave Scanning Radiometer (AMSR-E) on 7 May 2008. The positions of the moorings used for satellite ice motion data validation are indicated by black stars. The picture is taken from (Krumpfen et al., 2012).

Surface energy balance

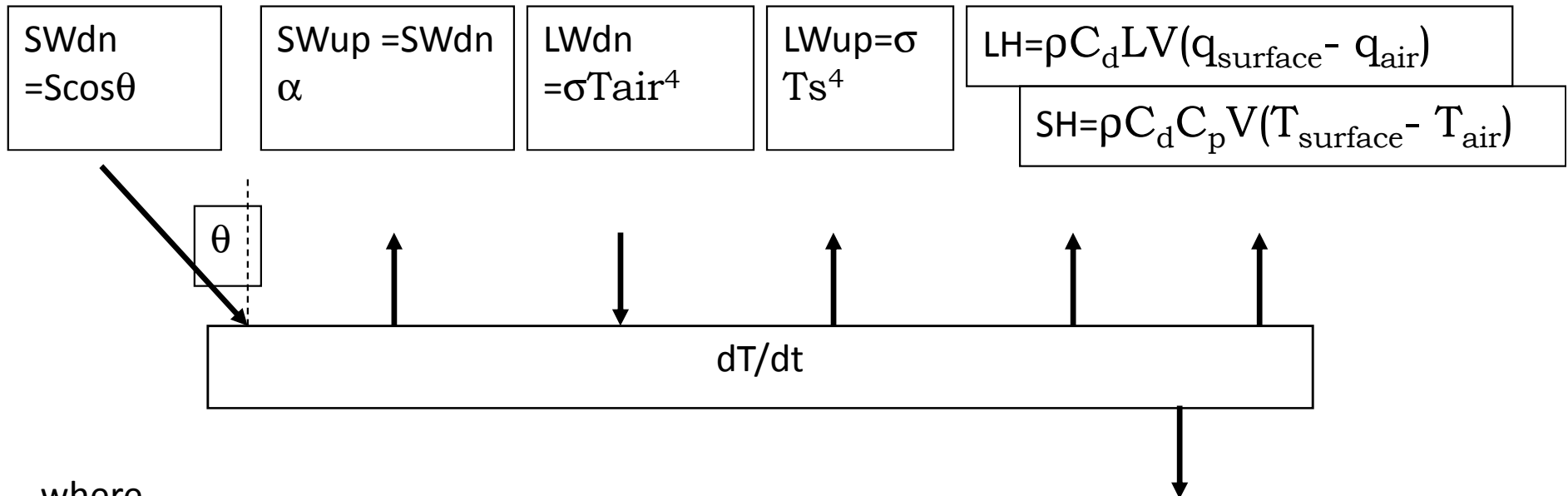
Incoming shortwave + Incoming longwave = Reflected shortwave + Emitted longwave
+ Latent heat flux + Sensible heat flux + Subsurface conduction



Albedo is the ratio of reflected radiation from the surface to incident radiation upon it

Summary: Surface energy balance

Incoming shortwave + Incoming longwave = Reflected shortwave + Emitted longwave
 + Latent heat flux + Sensible heat flux + Subsurface conduction



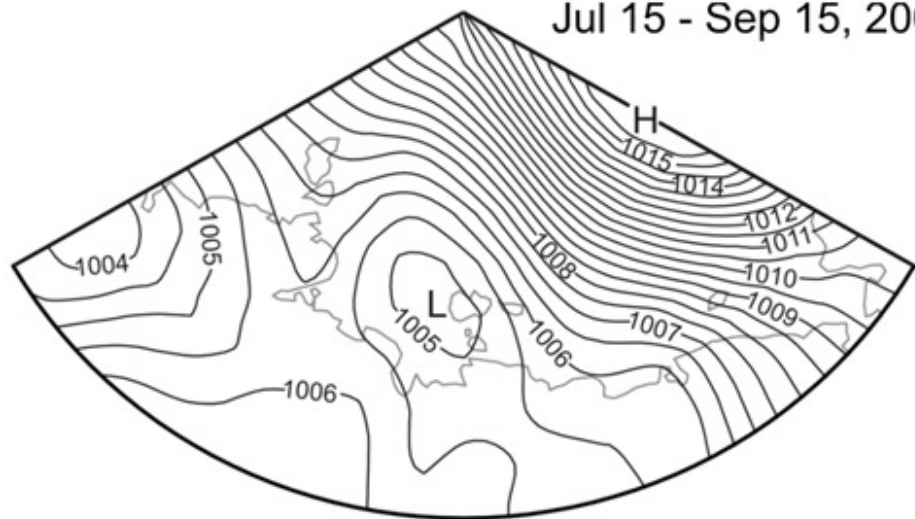
where

S is solar constant $S=1366 \text{ Watts/m}^2$

θ is solar zenith angle, which is the angle between the local zenith and the line of sight to the sun

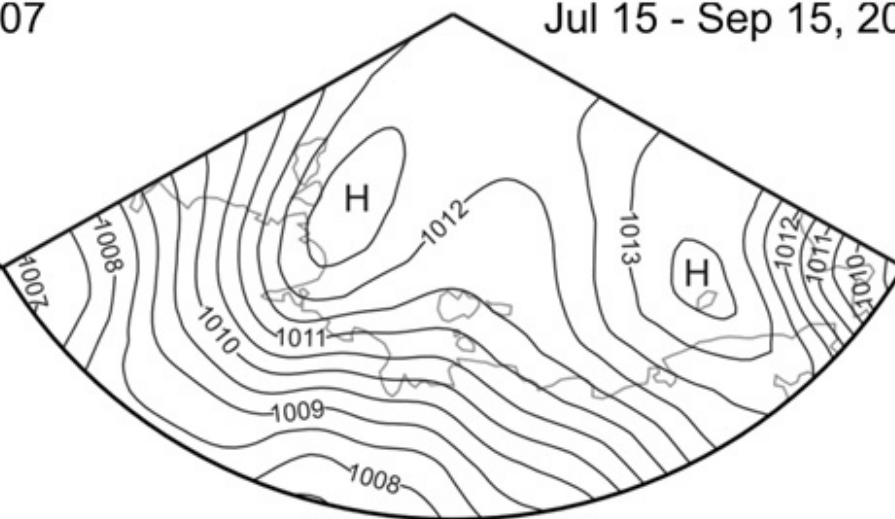
a

Jul 15 - Sep 15, 2007



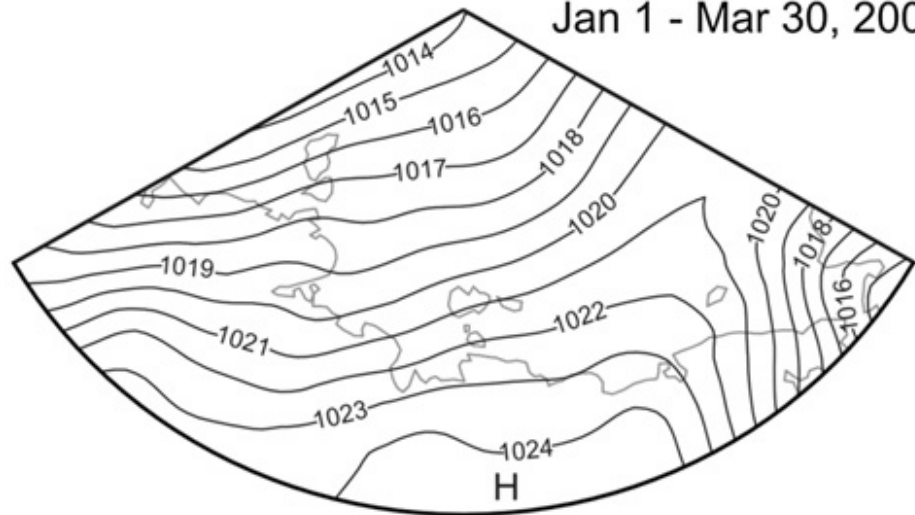
b

Jul 15 - Sep 15, 2008



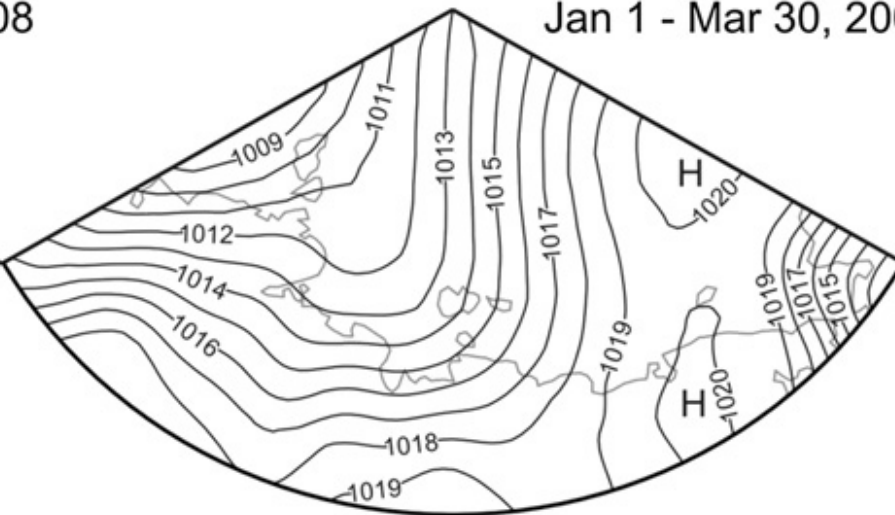
c

Jan 1 - Mar 30, 2008



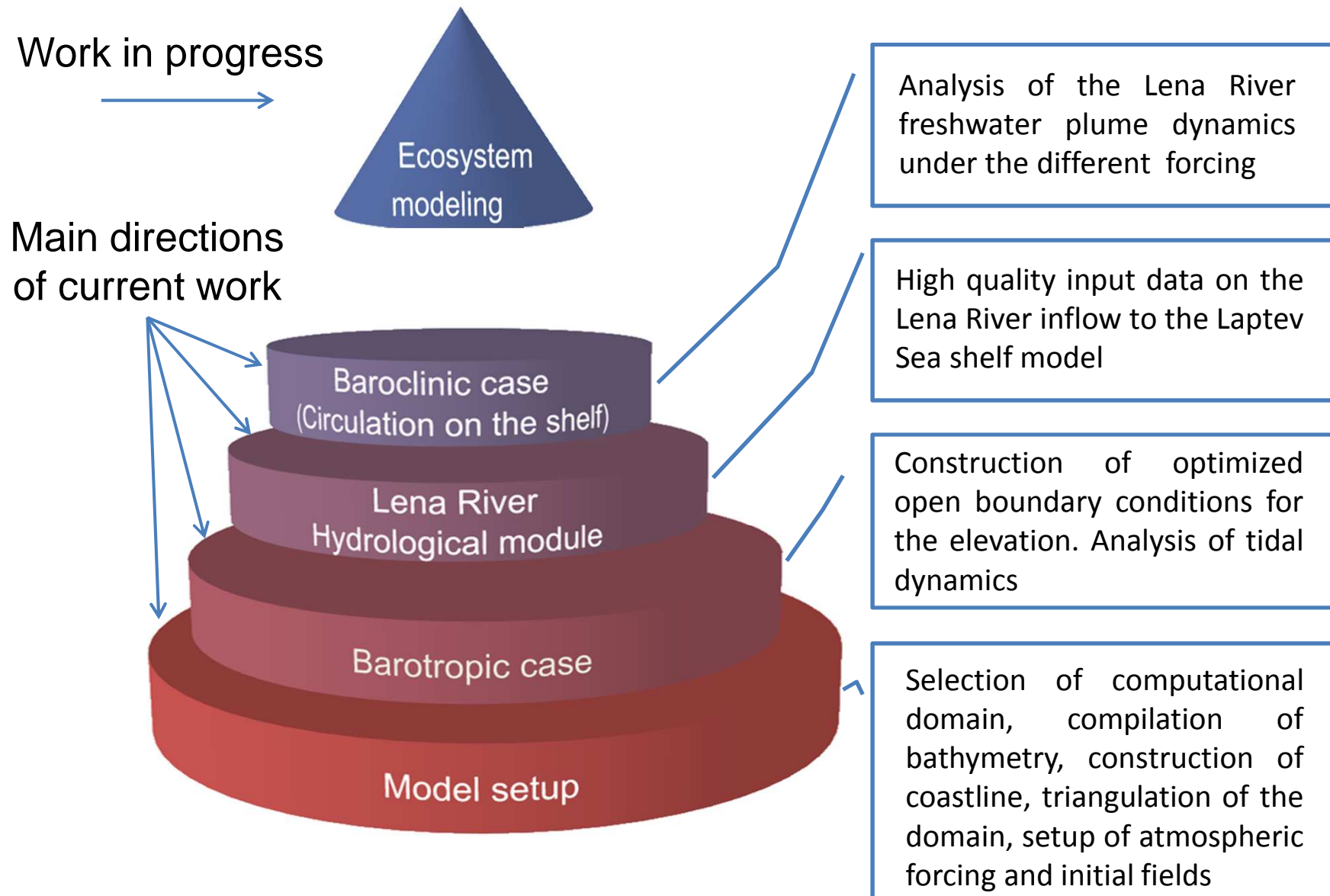
d

Jan 1 - Mar 30, 2009

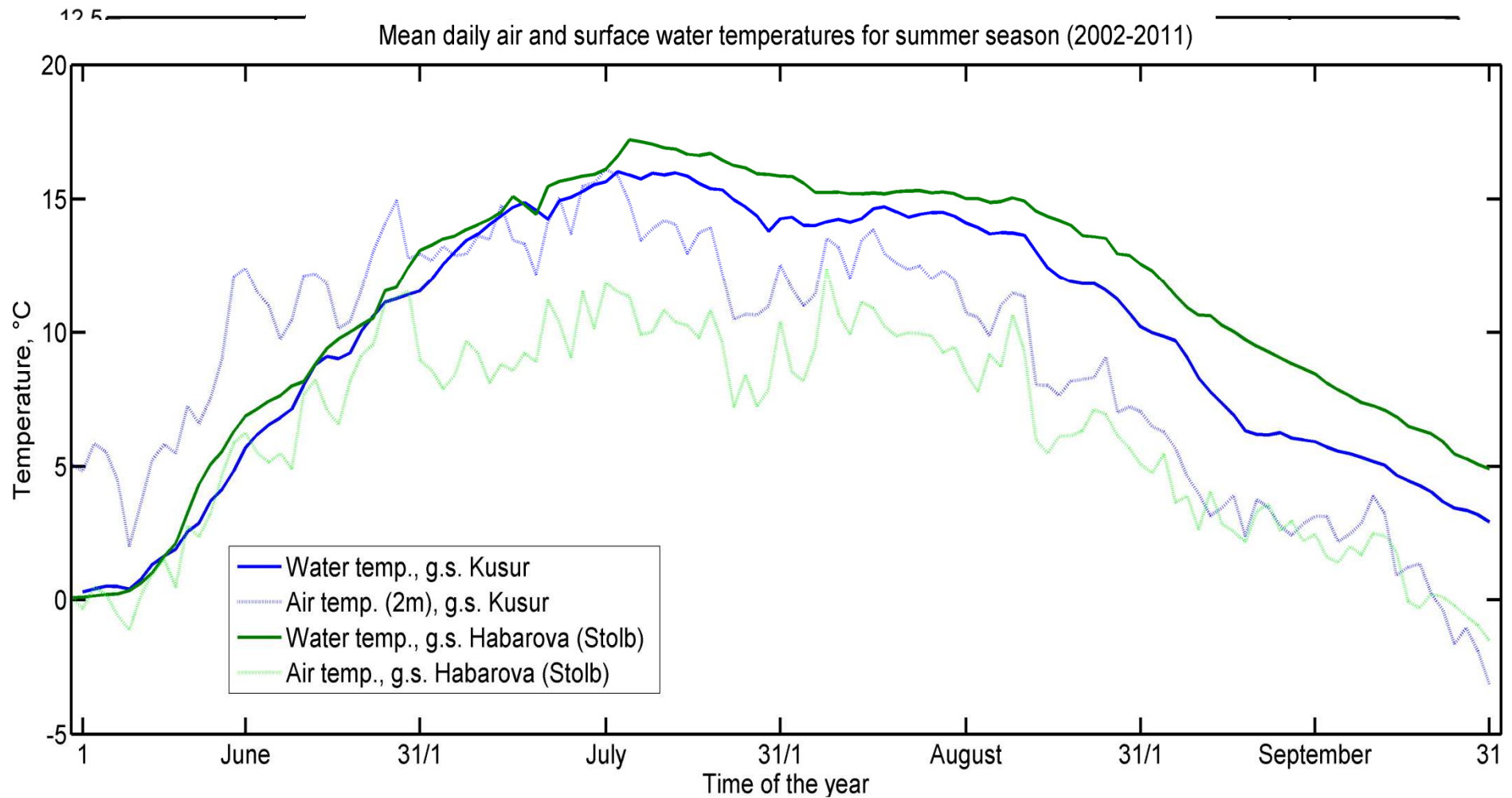


Main working steps

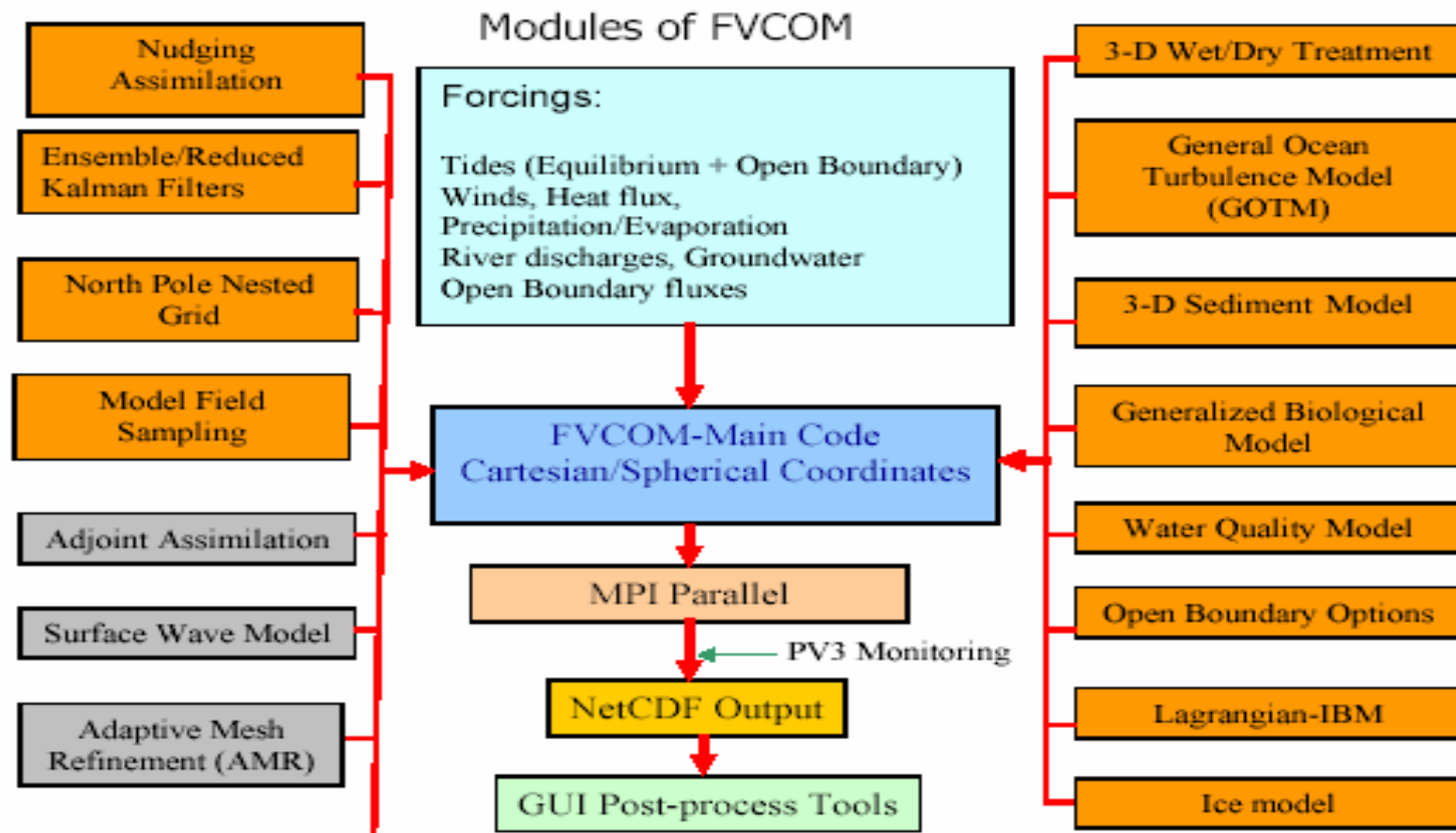
Main objectives of each stage



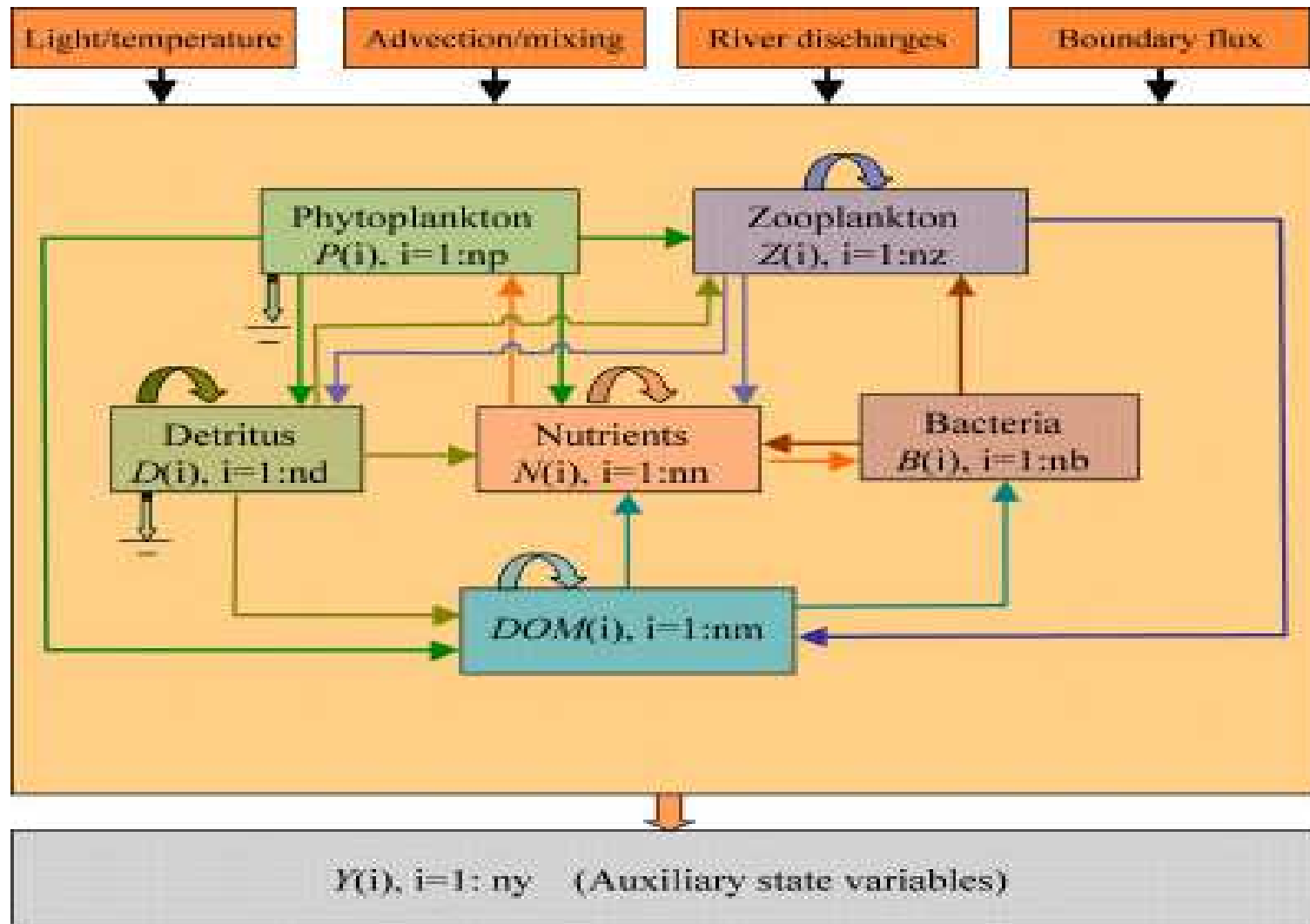
Kusur-Habarova (Stolb) surface water temperature anomaly



Schematic of FVCOM module structure

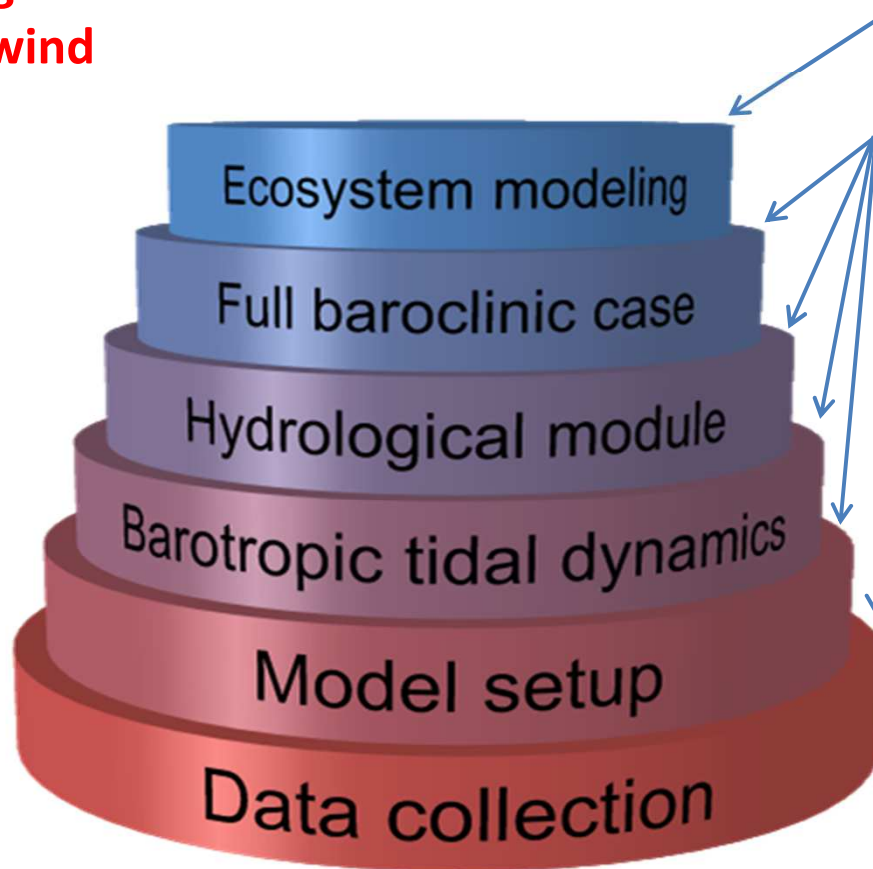
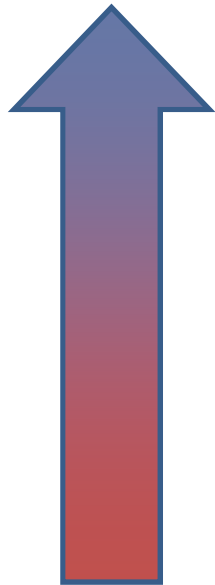


Flexible Biological Module



Workflow

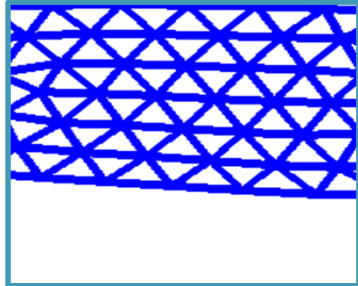
**Investigation of the Lena
River freshwater propagation
under the influence of wind
and tides**



Work in progress

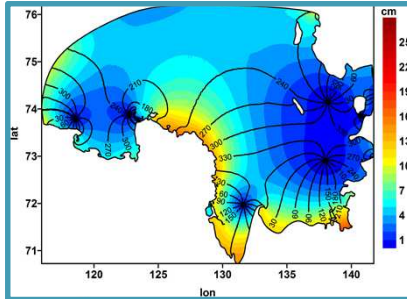
**Main directions
of current work**

I. Model setup



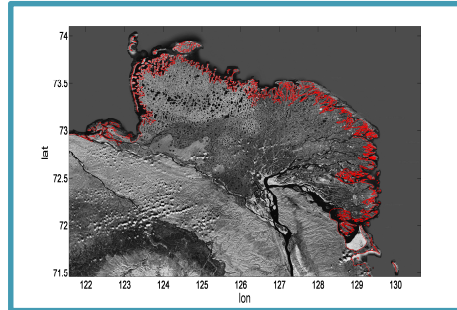
- Selection of computational domain
- Compilation of bathymetry
- Triangulation of the selected area
- Porting of FVCOM
- Setup of atmospheric forcing and initial fields

II. Barotropic tidal dynamics



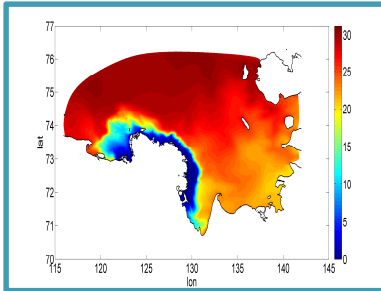
- Comparison of available tidal solutions
- Construction of optimized open boundary condition
- Construction of tidal maps for main tidal components
- Sensitivity study to additional bathymetric data
- Analysis of tidal ellipses and comparison with observations
- Analysis of residual circulation, energy fluxes and energy budget

III. Lena River hydrological module



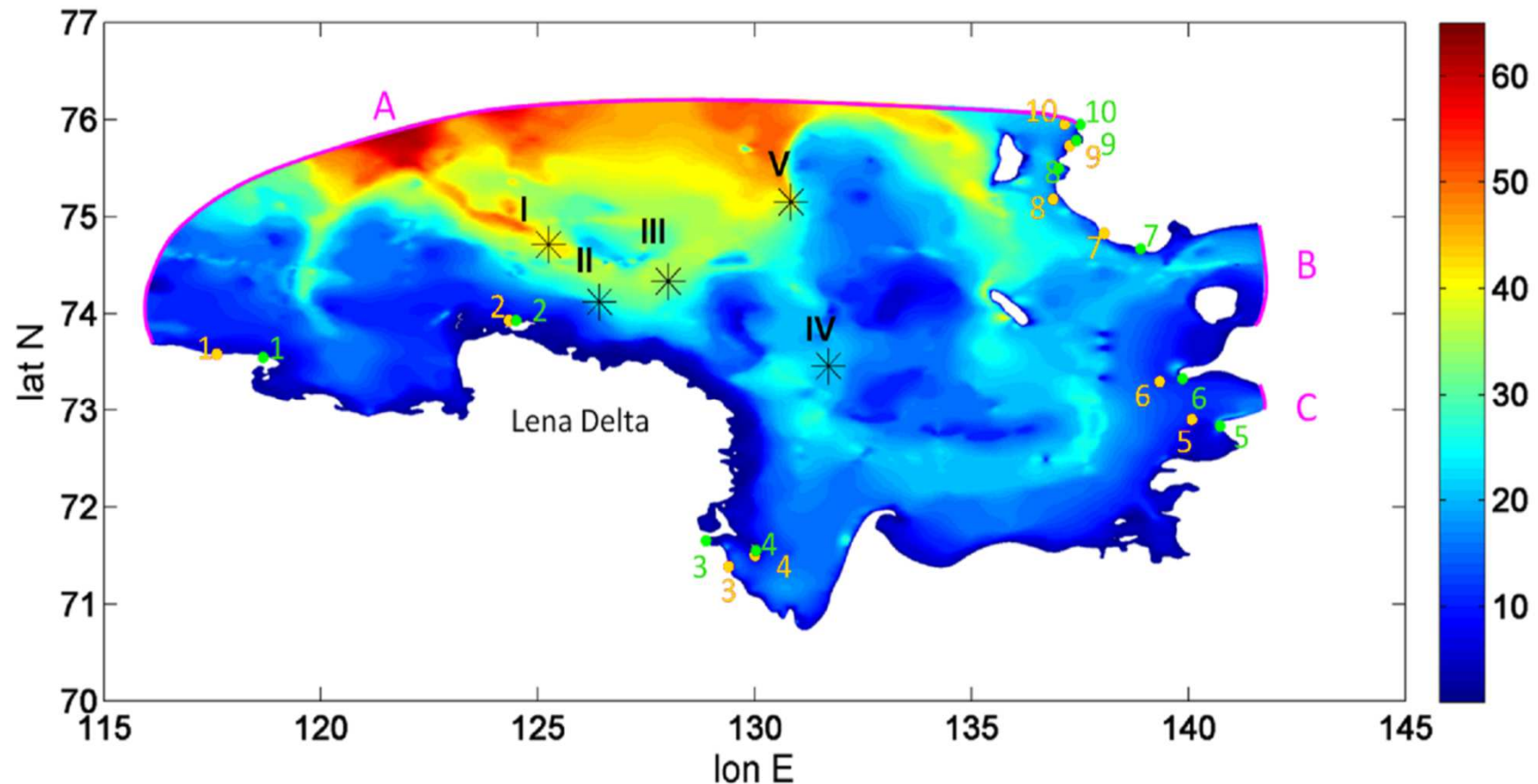
- Analysis of hydrologic trends in the Lena River basin outlet
- Description and analysis of water temperature anomaly found in the Lena Delta head area
- Modeling of the Lena River stream temperature using nonlinear regression
- Creating the Lena River hydrological module

IV. Baroclinic dynamics



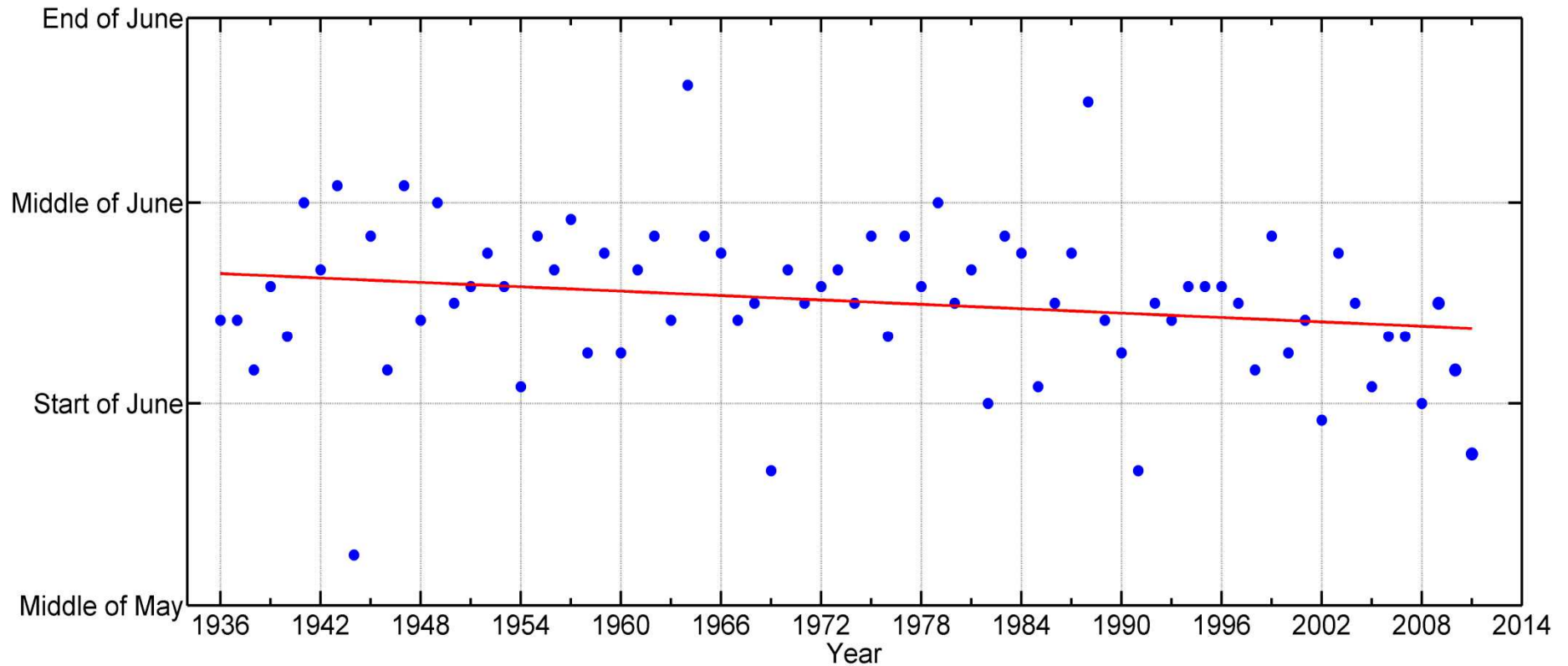
- Study of the impact of tides and winds on the Lena freshwater plume propagation in the region
- Study of the mixing processes in the region
- Comparison of different atmospheric forcing products
- Comparison of simulations against observations

Domain under consideration and available observational data



Bathymetry --- GEBCO, resolution ~ 2.5 km, and Soviet digitized map, resolution ~ 0.8 km; Tide gauges --- green and yellow dots, numbered; AWI moorings ---- asterisks; A, B and C --- open boundary segments

Lena River Hydrology



Time of the year when the daily flow of Lena reaches a maximum. Total annual discharge. The slope of the line is significantly different from 0 with **99.6% probability**. The slope of the line is significantly different from 0 with **94.1% probability**.

27.08.2014